

NACA RM L50L08

RESTRICTED

Copy 226
RM L50L08

NACA

RESEARCH MEMORANDUM

SPIN-TUNNEL INVESTIGATION OF A MODEL OF A SWEEP-WING
FIGHTER AIRPLANE OVER A WIDE RANGE OF
FUSELAGE-HEAVY LOADINGS

By Theodore Berman

Langley Aeronautical Laboratory
Langley Field, Va.

CLASSIFICATION CHANGED TO
CONFIDENTIAL
BY AUTHORITY J. W. CROWLEY
CHANGE #1739 DATE 12-11-53 T.C.F.

CLASSIFIED DOCUMENT

This document contains classified information affecting the National Defense of the United States within the meaning of the Espionage Act, USC 50:31 and 32. Its transmission or the revelation of its contents in any manner to an unauthorized person is prohibited by law.

Information so classified may be imparted only to persons in the military and naval services of the United States, appropriate civilian officers and employees of the Federal Government who have a legitimate interest therein, and to United States citizens of known loyalty and discretion who of necessity must be informed thereof.

CLASSIFICATION CHANGED TO UNCLASSIFIED

AUTHORITY: J.W. CROWLEY DATE: 10-29-54

CHANGE NO. 2317 WHL

NATIONAL ADVISORY COMMITTEE FOR AERONAUTICS

WASHINGTON
December 27, 1950

RESTRICTED

NATIONAL ADVISORY COMMITTEE FOR AERNAUTICS

RESEARCH MEMORANDUM

SPIN-TUNNEL INVESTIGATION OF A MODEL OF A SWEEP-WING
FIGHTER AIRPLANE OVER A WIDE RANGE OF
FUSELAGE-HEAVY LOADINGS

By Theodore Berman

SUMMARY

As part of a general program to extend the existing spin-recovery criterion, an investigation has been conducted to determine the spin and recovery characteristics and the tail-design requirements for satisfactory recovery through an extremely wide range of fuselage-heavy loadings of a model representative of a swept-wing fighter airplane.

The results showed that, as the loading of the model was changed so that the inertia yawing-moment parameter was increased negatively beyond -200×10^{-4} , the tail-damping power factor required for satisfactory recovery by rudder reversal alone increased from approximately 600×10^{-6} to some value between 1500×10^{-6} and 2000×10^{-6} . When the loadings of the model were such that the inertia yawing-moment parameters varied from approximately -650×10^{-4} to almost -1000×10^{-4} the model would not spin. For values of the inertia yawing-moment parameter between -1000×10^{-4} and -1600×10^{-4} , the tail-damping power factor required for satisfactory recovery was found again to be between 1500×10^{-6} and 2000×10^{-6} for recovery by rudder reversal alone. Further investigation showed that movement of the ailerons to neutral or with the spin simultaneously with rudder reversal was the most effective control manipulation for recovery and, for this design, resulted in satisfactory recovery characteristics over the entire range of values of the inertia yawing-moment parameter tested even for a tail-damping power factor of 0. Variation of the relative density from 25 to 35 caused no appreciable change in spin or recovery characteristics.

INTRODUCTION

The present spin-recovery design criterion (reference 1) covers a comparatively narrow range of loadings and current airplane models frequently fall outside this range; thus, prediction of the spin and

recovery characteristics of such designs without model tests is difficult. For example, some fighter-airplane designs are loaded extremely heavily along the fuselage and have swept and short-span wings so that the ranges of loadings and of the inertia yawing-moment parameter are much wider than in the past. The purpose of spinning research is the determination of spin and recovery characteristics of airplanes merely by examination of their mass and dimensional characteristics. As part of a general program to extend the existing spin-recovery criterion, therefore, an investigation was undertaken in the Langley 20-foot free-spinning tunnel to determine the spin and recovery characteristics and the tail-design requirements for satisfactory recovery for a model representative of a swept-wing fighter airplane for a wide range of fuselage-heavy loadings.

The present investigation included variation of the inertia yawing-moment parameter from -205×10^{-4} to -1571×10^{-4} and variation of the tail-damping power factor from 0 to 2020×10^{-6} for a constant center-of-gravity location and relative density. Most of the tests were made at a relative density of 25 but the effects of increasing the relative density to 35 were also investigated. A few tests were made in which the center-of-gravity location was varied.

SYMBOLS

b	wing span, feet
S	wing area, square feet
c	wing or elevator chord at any station along span
\bar{c}	mean aerodynamic chord, feet
x/\bar{c}	ratio of distance of center of gravity rearward of leading edge of mean aerodynamic chord to mean aerodynamic chord
z/\bar{c}	ratio of distance between center of gravity and fuselage reference line to mean aerodynamic chord (positive when center of gravity is below fuselage reference line)
m	mass of airplane, slugs
I_x, I_y, I_z	moments of inertia about X, Y, and Z body axes, respectively, slug-feet ²
$\frac{I_x - I_y}{mb^2}$	inertia yawing-moment parameter

$\frac{I_Y - I_Z}{mb^2}$	inertia rolling-moment parameter
$\frac{I_Z - I_X}{mb^2}$	inertia pitching-moment parameter
ρ	air density, slugs per cubic foot
μ	relative density of airplane ($m/\rho S b$)
α	angle between fuselage reference line and vertical (approximately equal to absolute value of angle of attack at plane of symmetry), degrees
ϕ	angle between span axis and horizontal (positive when right wing down), degrees
V	full-scale true rate of descent, feet per second
Ω	full-scale angular velocity about spin axis, revolutions per second
TDPF	tail-damping power factor ($TDR \times URVC$) (see reference 1)
TDR	tail-damping ratio
URVC	unshielded-rudder volume coefficient
σ	helix angle, angle between flight path and vertical, degrees

APPARATUS AND METHODS

Model

The model used for the present investigation was considered representative of a $\frac{1}{24}$ -scale model of a modern swept-wing fighter airplane. A three-view drawing of the model as tested with the normal tail is shown as figure 1. Figure 2 shows photographs of the model with the normal tail and figure 3 shows the tail modifications by means of which the value of tail-damping power factor was changed. The dimensional characteristics of the model scaled up to airplane values are presented in table I.

The model was ballasted to obtain dynamic similarity to an airplane at 15,000 feet ($\rho = 0.001496$ slug/cu ft). A remote-control mechanism was installed in the model to actuate the controls for the recovery attempts and sufficient moment was exerted on the controls during the recovery attempts to reverse them fully and rapidly.

Wind-Tunnel and Testing Technique

The tests were performed in the Langley 20-foot free-spinning tunnel, the operation of which is, in general, similar to that described in reference 2 for the Langley 15-foot free-spinning tunnel, except that the model launching technique has been changed. The model is now launched by hand into the vertically rising air stream with the controls set in the desired position. The airspeed is adjusted until it balances the weight of the model and, after a number of turns in the established spin, recovery is attempted by moving one or more controls by means of the remote-control mechanism. After recovery the model dives into a safety net. A photograph of the model spinning in the tunnel is shown as figure 4.

The spin data presented were converted to corresponding full-scale values by methods described in reference 2. The turns for recovery are measured from the time the controls are moved to the time the spin rotation ceases and the model dives into the net. For the spins which had a rate of descent in excess of that which can be attained in the tunnel, the rate of descent was recorded as greater than the velocity at the time the model hit the safety net, for example, >300 . For these tests, the recovery was attempted before the model reached its final attitude and while the model was descending in the tunnel. Such results are conservative; that is, recoveries will not be so fast as when the model is in the final attitude. For recovery attempts in which the model struck the safety net while it was still in a spin, the recovery was recorded as greater than the number of turns from the time the controls were moved to the time the model struck the net, for example, >3 . A >3 -turn recovery, however, does not necessarily indicate an improvement over a >7 -turn recovery. For recovery attempts in which the model did not recover after 10 turns, the recovery was recorded as ∞ . When the model recovered without control movement with the rudder set with the spin, the result was recorded as "no spin."

Spin-tunnel tests are usually made to determine the spin and recovery characteristics of the model at the normal spinning control configuration (elevator full up, ailerons neutral, and rudder full with the spin) and at various other aileron-elevator control combinations including zero and maximum deflections. Recovery is generally attempted by rapid full rudder reversal. During this investigation, recoveries were sometimes attempted by simultaneous movement of the rudder and

aileron. Tests are also performed to evaluate the possible adverse effects on recovery of small deviations from the normal-control configuration for spinning. For this type of test, the ailerons are set at one-third of the full deflection in the direction conducive to slower recoveries and the elevator is set at two thirds its full-up deflection or full up, whichever is conducive to slower recoveries. Recovery is generally attempted by rapidly reversing the rudder from full with the spin to only two thirds against the spin or by rudder and elevator movement when it is thought that elevator movement will be effective. This control configuration and movement is referred to as the "criterion spin." For this model, recovery characteristics were considered satisfactory if recovery from this criterion spin occurred in $2\frac{1}{4}$ turns or less by reversal of the rudder or by the alternate technique of simultaneous movement of the rudder to against the spin and the ailerons to neutral or with the spin. This criterion has been adopted on the basis of full-scale airplane spin-recovery data and corresponding model test results.

PRECISION

The model test results presented are believed to be true values given by the model within the following limits:

α , degrees	± 1
ϕ , degrees	± 1
V, percent	± 5
Ω , percent	± 2
Turns for recovery	
Obtained from film	$\pm \frac{1}{4}$
Obtained from visual observation	$\pm \frac{1}{2}$

The preceding limits may have been exceeded for some of the spins in which it was difficult to control the model in the tunnel because of the high rate of descent or because of the wandering or oscillatory nature of the spin.

Comparison between model and full-scale results (reference 3) indicates that model tests satisfactorily predicted full-scale recovery characteristics approximately 90 percent of the time and for the remaining 10 percent of the time the model results were of value in predicting some of the details of the full-scale spins. The airplanes generally spun at an angle of attack closer to 45° than to the model angle of attack and at a higher altitude loss per revolution than the

model although the higher rate of descent was found to be associated with the smaller angle of attack whether of airplane or model.

The accuracy of measuring the weight and mass distribution of the model is believed to be within the following limits:

Weight, percent	±1
Center-of-gravity location, percent \bar{c}	±1
Moments of inertia, percent	±5

The controls were set with an accuracy of $\pm 1^\circ$.

TEST CONDITIONS

A summary of the conditions tested is presented in table II and the inertia parameters for the loadings tested on the model are plotted in figure 5.

The maximum control deflections used for most of the tests were:

Rudder, degrees	20 right, 20 left
Elevator, degrees	25 up, 15 down
Ailerons, degrees	20 up, 20 down

For a few tests the maximum deflections of the rudder were 30° right and 30° left. Intermediate control deflections were also used as shown in the charts. For all tests the model was in the clean condition (landing flaps and landing gear retracted and cockpit closed).

The tests included changes of the tail-damping power factor of the model and these changes were made by the methods shown in figure 3. A tail-damping power factor of 0 was obtained by cutting the original rudder along a 15° line from the rear tip of the horizontal tail and fixing the bottom part at neutral. In this manner the entire movable rudder area was left in a shielded region and the value of the unshielded-rudder volume coefficient (URVC) was reduced to 0. A tail-damping power factor of 622×10^{-6} was obtained by cutting the rudder so that an appropriate rudder area was unshielded. The original tail design had a tail-damping power factor of 1079×10^{-6} and this factor was increased to 1557×10^{-6} and 2020×10^{-6} by adding ventral fins 1 and 2, respectively; thus, the tail-damping ratio (TDR) was increased.

RESULTS AND DISCUSSION

The results of the tests are presented in charts 1 to 30 and figure 6. Right and left spins of the model were symmetrical and therefore the data are presented in terms of right spins only. Although not completely consistent, a trend toward larger helix angles (σ) was noted with increasingly negative values of the inertia yawing-moment parameter; the average value obtained was 5° .

The spin and recovery characteristics of the model for a value of $\frac{I_x - I_y}{mb^2}$ of -205×10^{-4} are presented in charts 1 to 3. This loading is within the range of loadings presented in reference 1 which presented, in effect, a criterion for satisfactory spin recovery. For the normal tail design (tail-damping power factor of 1079×10^{-6}) recoveries were satisfactory by rudder reversal and, for a tail-damping power factor of 0, recoveries were unsatisfactory. At a tail-damping power factor of 622×10^{-6} , which is just above the boundary for satisfactory recovery characteristics in reference 1, recoveries were not quite satisfactory for the normal rudder deflections of $\pm 20^\circ$ but were satisfactory for a rudder deflection of $\pm 30^\circ$. Inasmuch as a study of the designs upon which reference 1 is based showed that most of those designs incorporated rudder deflections of greater than $\pm 20^\circ$, the results presented in charts 1 to 3 are considered to show that at this loading the spin and recovery characteristics of this design are conventional. Ailerons set against the spin (stick left in a right spin) and elevator down settings were found to be detrimental to recovery as would be expected from a study of reference 4.

As the inertia yawing-moment parameter became more negative $\left(\frac{I_x - I_y}{mb^2} \text{ of } -394 \times 10^{-4}\right)$ changes were noted in the spin and recovery characteristics of the model. As shown in charts 4 to 7, when the ailerons were set full against the spin the spin motion showed a tendency to be wandering and somewhat oscillatory in roll and yaw. The main change, however, was that, with ailerons against the spin, recoveries became very slow so that recoveries from the criterion spin, by rudder reversal, were unsatisfactory for the normal tail and a value of tail-damping power factor between 1557×10^{-6} and 2020×10^{-6} , obtained by adding ventral fins 1 and 2, was necessary for satisfactory recovery.

An additional increase negatively of the inertia yawing-moment parameter $\left(\frac{I_x - I_y}{mb^2} \text{ of } -671 \times 10^{-4} \text{ and } -865 \times 10^{-4}\right)$ resulted in "no spins" for all control settings (charts 8 to 10). When the ailerons

were set against the spin the model motion became quite oscillatory in roll and yaw immediately after launching and the model rolled out of the spin. When the ailerons were neutral or with the spin, the model motion was not so oscillatory but the initial launching rotation damped quickly and the model nosed down and recovered from the spin without control movement. The factors causing the no spins were felt to be connected with the factors that cause oscillatory motions in the developed spin as described in reference 5.

Increasing the inertia yawing-moment parameter negatively to values of -1052×10^{-4} and -1571×10^{-4} resulted in generally less oscillation of the model and, for some control configurations, steady spins were obtained (charts 11 to 18). When spins were obtained, recoveries by rudder reversal alone were unsatisfactory for the normal tail configuration (tail-damping power factor of 1079×10^{-6}) and with ventral fin 1 added (tail-damping power factor 1557×10^{-6}) but were satisfactory with ventral fin 2 added (tail-damping power factor 2020×10^{-6}).

Throughout the range of loadings tested, setting the ailerons with the spin resulted in a steep nose-down attitude apparently below the stall at the plane of symmetry, but the model continued turning. The turning of the model appeared to be caused by the ailerons (aileron roll); brief tests were made in which the ailerons were moved to neutral after the model had entered this steep attitude. The model stopped rotating immediately and this result indicated that the turning motion was due to the ailerons. Accordingly, the aileron with spin attempts were recorded as a no spin and as a steep spin with rapid recovery for motion occurring without rudder reversal and after rudder reversal, respectively. Because of the high rate of descent of all spins when the ailerons were with the spin, the model could only be observed for limited lengths of time and all aileron with spins might have been no spins if they could have been observed in the tunnel longer.

The results for this design showed that for satisfactory recovery characteristics by rudder reversal over the complete range of loadings a value of tail-damping power factor larger than is normally found in present designs (between 1557×10^{-6} and 2020×10^{-6}) is necessary. This value was believed to be undesirably high and, if possible, some other recovery technique that would not require so high a value of tail-damping power factor for satisfactory recovery was believed to be desirable. The first recovery technique considered was movement of the elevator in conjunction with rudder reversal. Spin-tunnel experience has indicated that movement of the elevator down during the developed spin is beneficial to recovery when the loading is mainly along the wings (inertia yawing-moment parameter positive) but is of little effect when the loading is mainly along the fuselage. For the range of loadings of the present investigation, therefore, the elevator movement could not be expected to aid recovery substantially. Examination of the test data showed that,

for all loadings, when the ailerons were set with the spin, the model either did not spin or spun very steeply and recovered rapidly, whereas the slow recoveries were obtained when the ailerons were set against the spin. Recoveries were therefore attempted by simultaneous reversal of the rudder and movement of the ailerons to neutral or with the spin. As shown in the charts and in figure 6, this recovery technique was very effective. Although the results indicated that aileron reversal alone might not effect satisfactory recoveries, when the recovery technique of simultaneous movement of the rudder and ailerons was applied the tail-damping power factor required for satisfactory recovery was found to be 0. The apparent effectiveness of the rudder even with a tail-damping power factor of 0 may be explained by the fact that the attitude of aileron with spins was steeper than the attitude for which tail-damping power factor is computed and therefore part of the rudder may have been unshielded.

In the past, aileron movement has not been recommended to effect recovery, because movement of an additional control for recovery may cause the pilot to be confused, the variation of loading in flight quite often changed the direction of favorable aileron movement, and spin-tunnel tests had indicated that models were generally slow to respond to aileron movement. Most current designs, however, are so loaded (fuselage heavy) that, for the entire range of possible loadings, movement of the ailerons to with the spin would be favorable. For airplanes that have a very great part of their weight distributed along the fuselage relative to the weight in the wings, the response of the airplane to aileron movement during spins might be expected to be rapid because of inertia effects and, therefore, because the conventional recovery technique appeared to be inadequate, this new recovery technique is recommended. The effect of the aileron movement was to cause the right wing to move down (ϕ positive) and thereby, $\frac{I_x - I_y}{mb^2}$ being negative, to cause an antispin inertia yawing moment which in conjunction with the moment opposing the spin due to the rudder resulted in rapid recovery.

In analyzing the results, recoveries by rudder reversal alone in several instances varied from $1/2$ turn to ∞ for the same control configuration. Study of the films of these recoveries showed that, in such cases, the spin was oscillatory to some degree and, when the inner wing was above the horizon at the moment the rudder was reversed, recoveries were poor, but that, when the rudder was reversed when the inner wing was below the horizon (ϕ positive), recoveries were rapid. This result agrees with the previously mentioned results which indicated that moving the ailerons with the spin facilitates recovery.

A method of predicting the oscillatory motions of the model that sometimes resulted in no spin was shown in reference 5. This reference

indicated that increasing the inertia yawing-moment parameter negatively or increasing the side-area moment factor (approximately the ratio of the moment of the area forward of the center of gravity to the moment of the area rearward of the center of gravity) results in violently oscillatory motions. The trend towards oscillatory motions in this investigation was similar to that of reference 5 but the boundary between the oscillatory and steady regions was not the same. This shift in boundary is probably explained by the fact that all the designs in reference 5 had straight wings, whereas the present design has a swept wing. Inasmuch as the inertia yawing-moment parameter includes a wing span factor, the shorter spans of the swept wings result in relatively higher negative values of the inertia yawing-moment parameter. The aerodynamic characteristics of the swept wing may also cause a shift in the boundary. Reference 5 shows that, as the inertia yawing-moment parameter increased negatively, oscillatory motions occurred at lower side-area moment factors. The data presented herein agree with reference 5 for the same range of values of the inertia yawing-moment parameter, but, as the values of the inertia yawing-moment parameter were increased further negatively, oscillations occurred only with larger values of side-area moment factor.

Effect of Change of Relative Density

The data discussed hitherto were obtained with the model loaded to represent a value of μ of 25. Corresponding data obtained when the model was loaded to represent $\mu = 35$ are shown in charts 19 to 27. Comparison indicates that the change in μ had little effect on the spin and recovery characteristics of the model.

Analysis of the results presented in charts 25 to 27 for $\mu = 35$ and a value of the inertia yawing-moment parameter of -997×10^{-4} and comparison with corresponding results at $\mu = 25$ (charts 11 to 13) indicate that, if tests had been conducted, unsatisfactory recoveries would have been obtained for spins with ailerons one third against the spin and elevator full up for tail-damping power factor of 0 and 1079×10^{-6} (charts 25 and 26).

Effect of Change of Center-of-Gravity Location

Data presented in charts 28 to 30 are the results of brief tests previously mentioned in which the center-of-gravity location was varied with loadings 1 and 3 as basic loadings. These data show that when the center-of-gravity location was moved forward from loading 3 (x/\bar{c} from 0.198 to 0.110) while the inertia parameters about the center of gravity were held approximately constant (chart 28) the spins became less

oscillatory and spins were obtained at control configurations at which the model had not spun previously. This effect was consistent with the data of reference 5, inasmuch as movement of the center-of-gravity forward reduced the side-area moment factor.

Movement of the center-of-gravity location rearward of normal from loading 3 (x/\bar{c} from 0.198 to 0.393) while keeping the inertia parameters approximately constant (chart 29) also resulted in a tendency toward less oscillation and more steady spins than were obtained at the basic loading. Based on side-area moment factor alone, this effect was not expected and other changes such as the decrease in tail-damping power factor associated with the rearward center-of-gravity movement appear to account partially for the result obtained. Tests made with the center-of-gravity location moved rearward from loading 1 (x/\bar{c} from 0.194 to 0.399) while keeping the inertia parameters approximately constant (chart 30), a loading which is in the range of inertia yawing-moment parameters previously investigated and reported upon in reference 5, however, showed a trend similar to that of reference 5 (rearward movement of the center of gravity caused more oscillatory spins and, for aileron-against settings, recoveries were improved because of the oscillations).

Extended Spin-Recovery Criterion

A first approximation of the extended spin-recovery criterion is presented in figure 6. Because this figure is based on only one basic configuration, the boundaries shown are approximate and apply only to designs similar to the design tested, but the trends for spin characteristics shown and for control techniques necessary for satisfactory recovery should apply generally.

CONCLUSIONS

Based on the results of the present investigation which was intended as part of a general investigation to determine the tail-design requirements for satisfactory recovery through an extremely wide range of fuselage-heavy loadings in order to extend the existing spin-recovery criterion, the following conclusions were drawn which are believed to apply to designs similar to the model tested and to show general trends in spin characteristics and control techniques required for satisfactory recovery:

1. Increasing the inertia yawing-moment parameter negatively beyond -200×10^{-4} to approximately -650×10^{-4} increased the tail-damping power factor required for satisfactory recovery by rudder reversal alone

from a value of approximately 600×10^{-6} to a value between 1500×10^{-6} and 2000×10^{-6} .

2. Further negative increase of the inertia yawing-moment parameter indicated that between values of the parameter of -650×10^{-4} and -1000×10^{-4} spins could not be obtained and that, at least in part, the no spins were due to the same factors that normally lead to oscillatory motions in spinning attitudes.

3. For values of inertia yawing-moment parameter between -1000×10^{-4} and -1600×10^{-4} the value of the tail-damping power factor required for satisfactory recovery by rudder reversal alone was between 1500×10^{-6} and 2000×10^{-6} .

4. Movement of the ailerons with the spin simultaneously with rudder reversal was the most effective control manipulation for recovery from spins and resulted in satisfactory recovery characteristics over the entire range of inertia yawing-moment parameter tested even for a tail-damping power factor of 0.

5. Variation of relative density from 25 to 35 caused no appreciable change in spin or recovery characteristics.

Langley Aeronautical Laboratory
National Advisory Committee for Aeronautics
Langley Field, Va.,

REFERENCES

1. Neihouse, Anshal I., Lichtenstein, Jacob H., and Pepoon, Philip W.: Tail-Design Requirements for Satisfactory Spin Recovery. NACA TN 1045, 1946.
2. Zimmerman, C. H.: Preliminary Tests in the N.A.C.A. Free-Spinning Wind Tunnel. NACA Rep. 557, 1936.
3. Berman, Theodore: Comparison of Model and Full-Scale Spin Test Results for 60 Airplane Designs. NACA TN 2134, 1950.
4. Neihouse, A. I.: A Mass-Distribution Criterion for Predicting the Effect of Control Manipulation on the Recovery From a Spin. NACA ARR, Aug. 1942.
5. Stone, Ralph W., and Klinar, Walter J.: The Influence of Very Heavy Fuselage Mass Loadings and Long Nose Lengths upon Oscillations in the Spin. NACA TN 1510, 1948.

TABLE I.- DIMENSIONAL CHARACTERISTICS OF THE MODEL SCALED UP TO
AIRPLANE VALUES BASED ON AN ASSUMED SCALE OF 1/24

Length over-all, ft	54.25
Normal center-of-gravity location, percent \bar{c}	19.6
Wing:	
Span, ft	39.67
Area, sq ft	350
Sweepback at $c/4$, deg	35
Incidence, deg	1
Dihedral, deg	0
Section	NACA 65-009
Aspect ratio	4.50
Mean aerodynamic chord, ft	9.8
Leading edge of \bar{c} rearward of leading edge of root chord, ft	6.8
Ailerons:	
Area, sq ft	18.4
Span, percent $b/2$	37.8
Hinge-line location, percent c	75
Horizontal tail surfaces:	
Total area, sq ft	66.8
Span, ft	15.3
Elevator area rearward of hinge line, sq ft	15.6
Distance from normal center of gravity to elevator hinge line at fuselage center line, ft	26.6
Incidence, deg	0
Sweepback, deg	35
Vertical tail surfaces:	
Total area, sq ft	46.6
Total rudder area rearward of hinge line, sq ft	10.7
Distance from normal center of gravity to rudder hinge line at water line 70 (70 in. above water line 0) ft	27.7



TABLE II.- MASS CHARACTERISTICS, INERTIA PARAMETERS, AND TAIL DAMPING POWER FACTORS FOR
THE LOADINGS TESTED WITH A MODEL OF A SWEEP-WING AIRPLANE

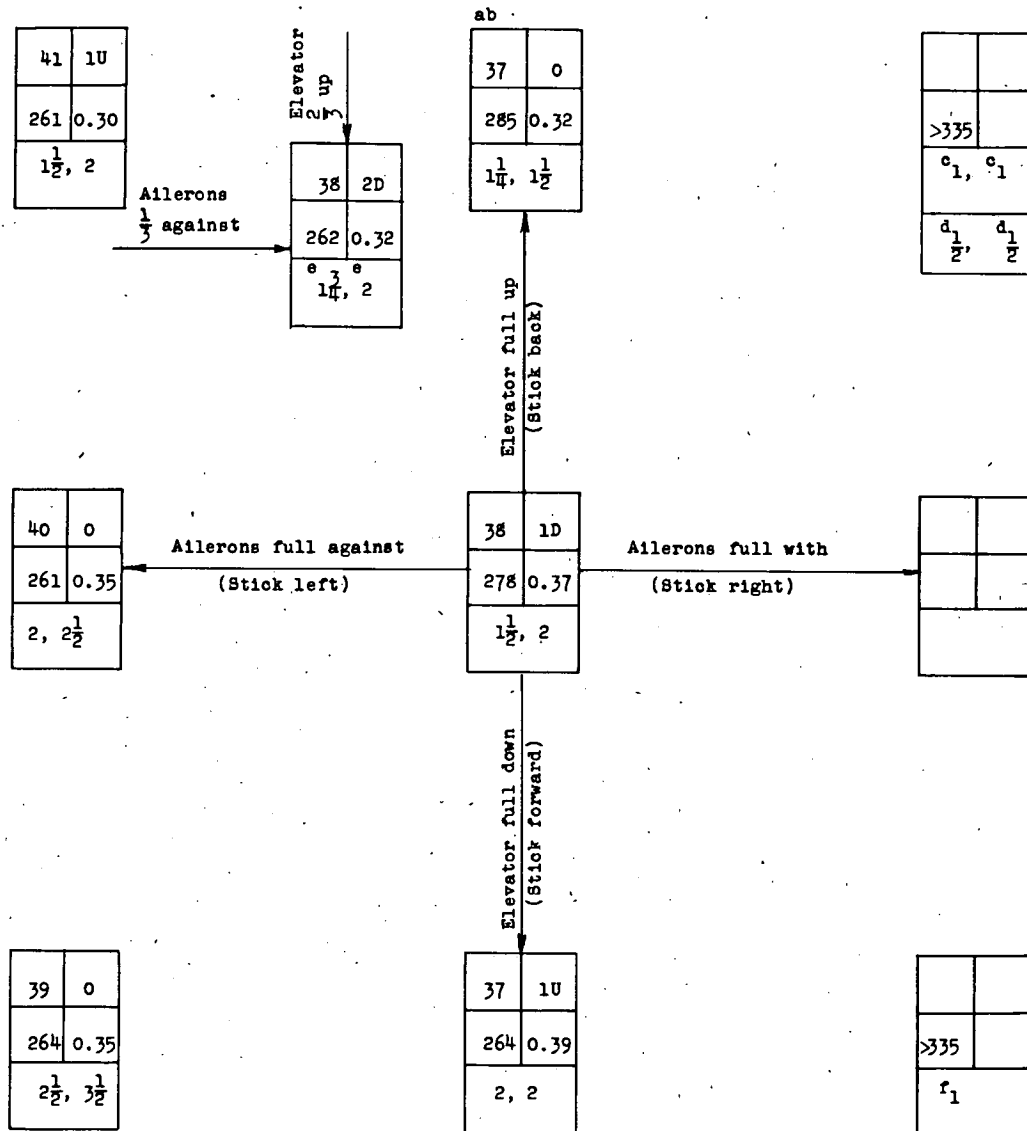
[Values given as corresponding full-scale values of a $\frac{1}{24}$ -scale model; moments of inertia are given about center of gravity.]

Loading	Weight (lb)	Center-of-gravity location		Relative density, μ at 15,000 feet	Moments of inertia (slug-ft ²)			Mass parameters			TDPF	Chart presenting data
		x/ \bar{c}	z/ \bar{c}		I _x	I _y	I _z	$\frac{I_x - I_y}{mb^2}$	$\frac{I_y - I_z}{mb^2}$	$\frac{I_z - I_x}{mb^2}$		
1	16,715	0.194	-0.040	25.0	30,516	47,285	75,747	-205 $\times 10^{-4}$	-348 $\times 10^{-4}$	554 $\times 10^{-4}$	1079 $\times 10^6$	1
	16,715	.194	.040	25.0	30,516	47,285	75,747	-205	-348	554	622	2
	16,715	.194	.040	25.0	30,516	47,285	75,747	-205	-348	554	0	3
2	16,801	.196	.040	25.1	17,374	49,764	64,302	-394	-177	571	2020	4
	16,801	.196	.040	25.1	17,374	49,764	64,302	-394	-177	571	1557	5
	16,801	.196	.040	25.1	17,374	49,764	64,302	-394	-177	571	1079	6
	16,801	.196	.040	25.1	17,374	49,764	64,302	-394	-177	571	0	7
3	16,667	.198	.064	24.9	16,821	71,511	85,769	-671	-175	846	1079	8
	16,667	.198	.064	24.9	16,821	71,511	85,769	-671	-175	846	0	9
4	16,743	.199	.066	25.0	17,036	87,842	102,654	-865	-178	1046	1079	10
5	16,897	.197	.068	25.3	7,362	94,283	98,692	-1052	-53	1106	2020	11
	16,897	.197	.068	25.3	7,362	94,283	98,692	-1052	-53	1106	1557	12
	16,897	.197	.068	25.3	7,362	94,283	98,692	-1052	-53	1106	1079	13
	16,897	.197	.068	25.3	7,362	94,283	98,692	-1052	-53	1106	0	14
6	16,815	.194	.092	25.2	7,369	136,474	140,493	-1571	-49	1620	2020	15
	16,815	.194	.092	25.2	7,369	136,474	140,493	-1571	-49	1620	1557	16
	16,815	.194	.092	25.2	7,369	136,474	140,493	-1571	-49	1620	1079	17
	16,815	.194	.092	25.2	7,369	136,474	140,493	-1571	-49	1620	0	18
7	23,276	.195	.021	34.8	36,995	60,690	95,345	-208	-305	513	1079	19
8	23,170	.202	.036	34.6	20,617	68,762	87,314	-425	-164	589	1079	20
9	23,161	.202	.042	34.6	20,648	91,648	109,898	-627	-161	788	1079	21
10	23,410	.216	.053	35.0	15,767	112,164	125,590	-843	-117	960	0	22
	23,410	.216	.053	35.0	15,767	112,164	125,590	-843	-117	960	1079	23
	23,410	.216	.053	35.0	15,767	112,164	125,590	-843	-117	960	1557	24
11	23,563	.194	.056	35.2	9,836	124,686	132,245	-997	-66	1063	0	25
	23,563	.194	.056	35.2	9,836	124,686	132,245	-997	-66	1063	1079	26
	23,563	.194	.056	35.2	9,836	124,686	132,245	-997	-66	1063	1557	27
12	16,954	.110	.055	25.3	7,164	58,095	62,623	-615	-55	669	1079	28
13	16,944	.393	.051	25.3	8,457	58,595	64,414	-605	-70	676	1079	29
14	16,720	.399	.068	25.0	32,964	46,688	78,140	-162	-382	550	1079	30

CHART 1.- SPIN AND RECOVERY CHARACTERISTICS OF THE MODEL AT LOADING 1 AND

A TAIL-DAMPING POWER FACTOR OF 1079×10^{-6}

$$\left[\frac{I_x - I_y}{mb^2} = -205 \times 10^{-4}, \mu = 25, \text{ recovery attempted by rapid full rudder reversal unless otherwise noted, right spins} \right]$$

^aWhipping spin.^bWandering spin.^cRecovery attempted before model reached final attitude. After rudder reversal model recovered by going into an aileron roll.^dRecovery attempted by simultaneous reversal of rudder and neutralization of ailerons. Model recovered in an erect dive.^eRecovery attempted by reversing rudder from full with to 2/3 against the spin.^fRecovery attempted before model in final attitude. Model recovered and then went into an inverted spin.

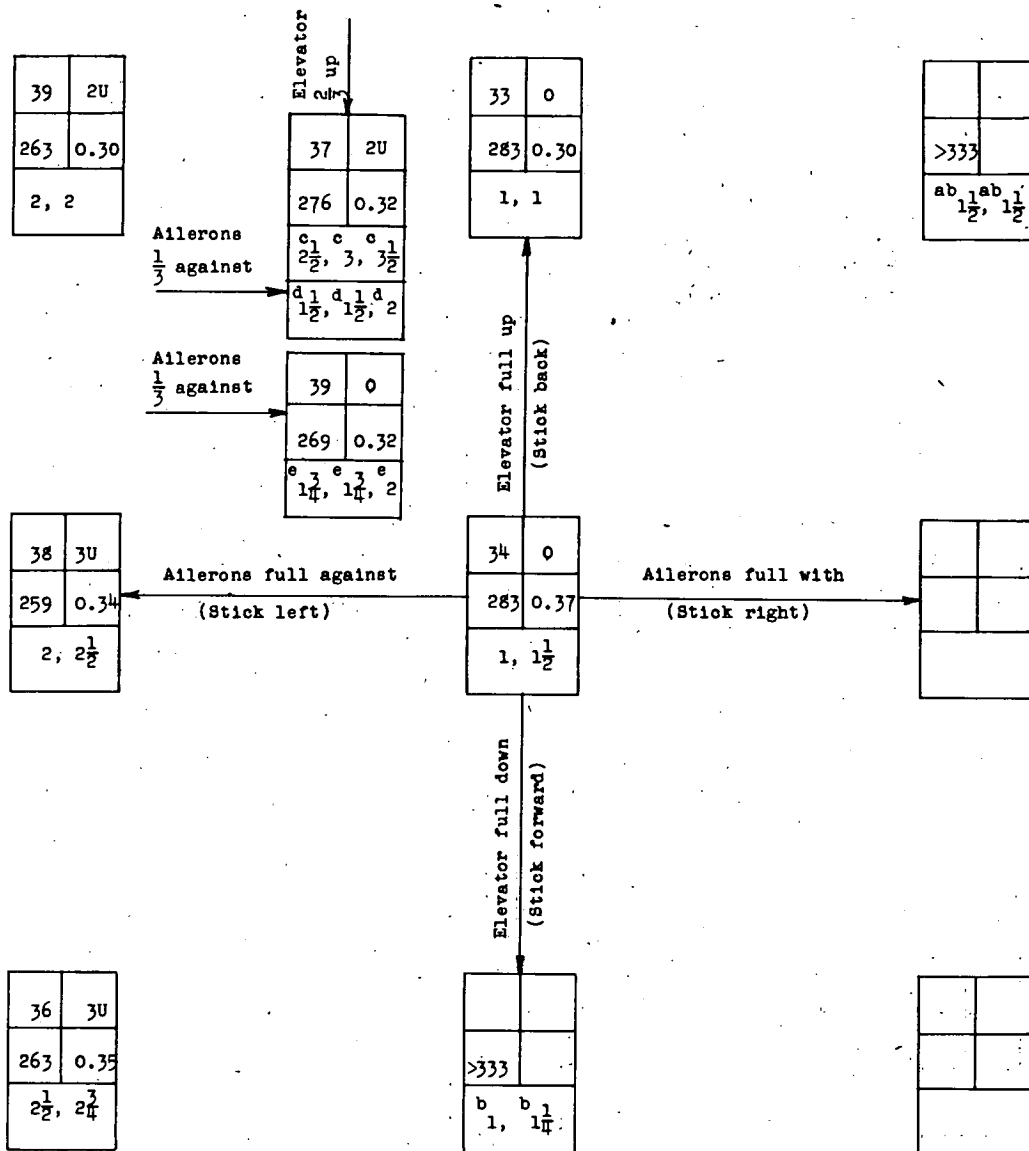
Model values converted to corresponding full-scale values.
 U inner wing up
 D inner wing down

a (deg)	φ (deg)
V (fps)	Ω (rps)
Turns for recovery	



CHART 2.- SPIN AND RECOVERY CHARACTERISTICS OF THE MODEL AT LOADING 1 AND
A TAIL-DAMPING POWER FACTOR OF 622×10^{-6}

$\frac{I_x - I_y}{mb^2} = -205 \times 10^{-4}$, $\mu = 25$, recovery attempted by rapid full rudder reversal unless
otherwise noted, right spins]



^aModel recovered by going into an aileron roll.

^bRecovery attempted before model reached final attitude.

^cRecovery attempted by reversing rudder from full with to $\frac{2}{3}$ against.

^dRecovery attempted by simultaneously reversing rudder from full with to $\frac{2}{3}$ against and

ailerons from $\frac{1}{3}$ against to neutral.

^eRecovery attempted by reversing rudder from 30° with the spin to 20° against the spin.

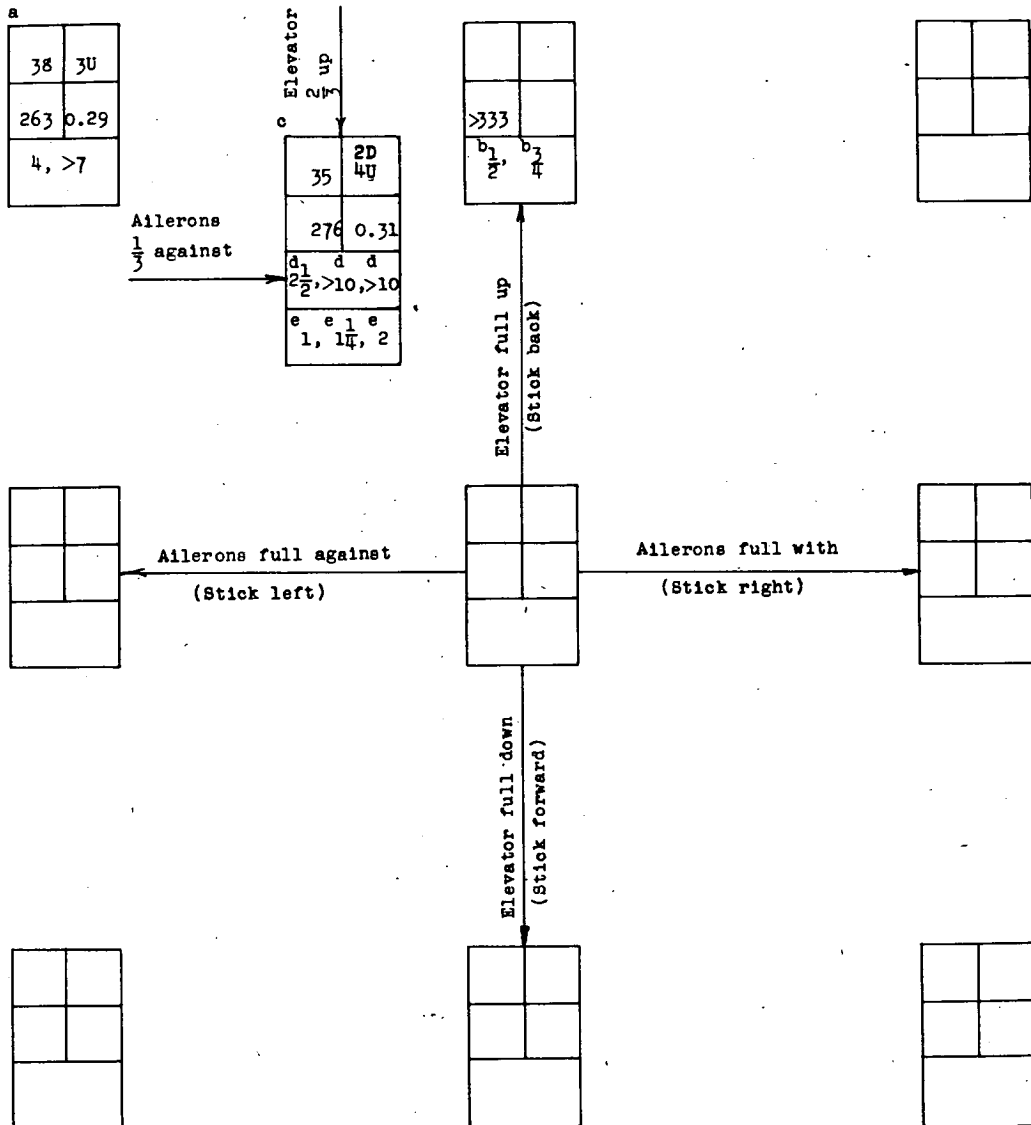
Model values converted to corresponding full-scale values.
U, inner wing up
D, inner wing down

α (deg)	ϕ (deg)
V (fps)	Ω (rps)
Turns. for recovery	

NACA

CHART 3.- SPIN AND RECOVERY CHARACTERISTICS OF THE MODEL AT LOADING 1
AND A TAIL-DAMPING POWER FACTOR OF 0

$\frac{I_x - I_y}{mb^2} = -205 \times 10^{-4}$, $\mu = 25$, recovery attempted by rapid full rudder reversal unless otherwise noted, right spins]



^aWandering spin.

^bRecovery attempted before model reached final attitude.

^cSomewhat oscillatory in roll and yaw, average values or range of values given.

^dRecovery attempted by reversing the rudder from full with to $\frac{2}{3}$ against the spin.

^eRecovery attempted by movement of rudder from full with to $\frac{2}{3}$ against and movement of the ailerons from $\frac{1}{3}$ against to neutral.

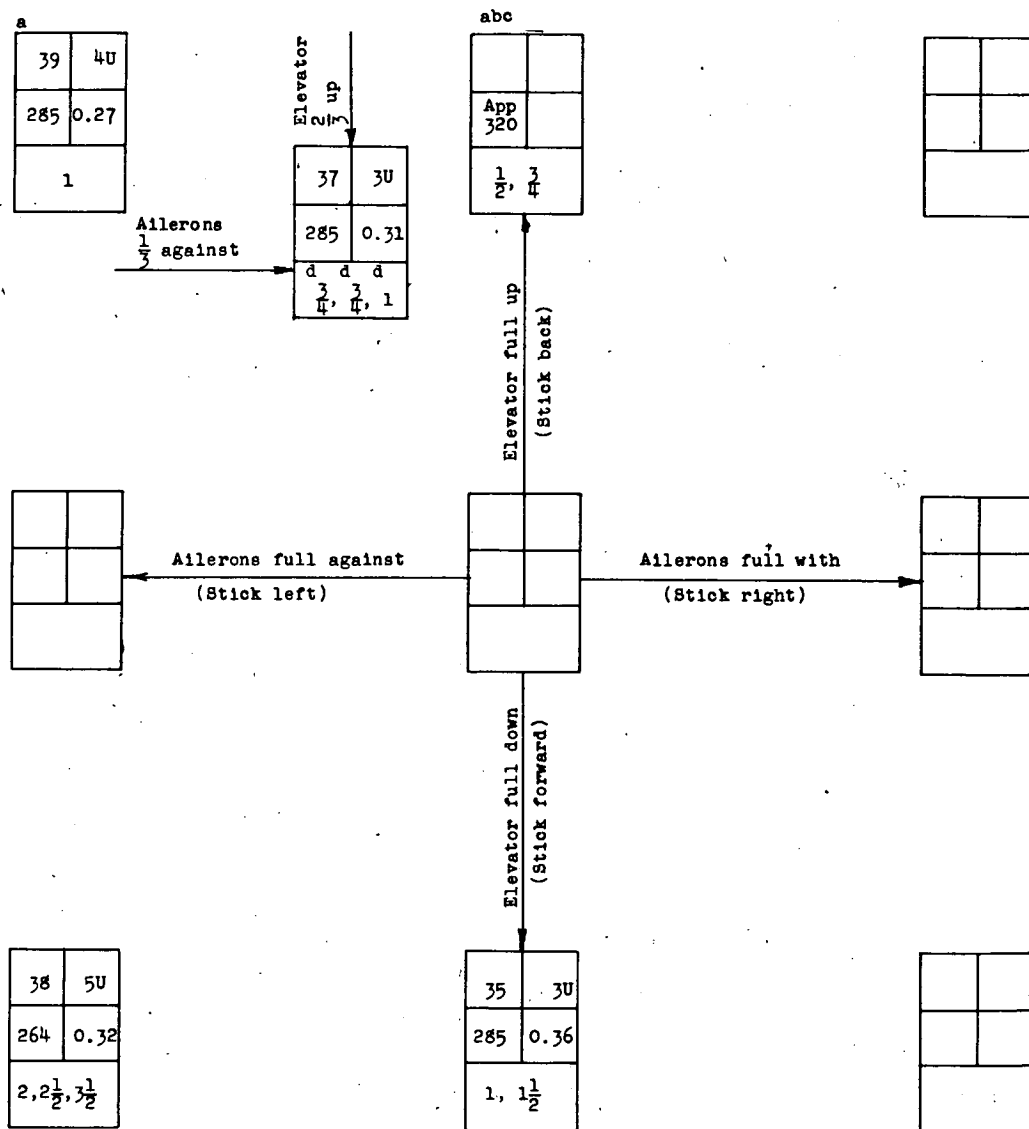
Model values converted to corresponding full-scale values.
U inner wing up
D inner wing down

α (deg)	ϕ (deg)
V (fps)	Ω (rps)
Turns for recovery	



CHART 4.- SPIN AND RECOVERY CHARACTERISTICS OF THE MODEL AT LOADING 2 AND
A TAIL-DAMPING POWER FACTOR OF 2020×10^{-6}

$$\left[\frac{I_x - I_y}{mb^2} = -394 \times 10^{-4}, \mu = 25, \text{ recovery attempted by rapid full rudder reversal unless otherwise noted, right spins} \right]$$



^aWandering spin.

^bWhipping spin.

^cRecovery attempted before model reached final attitude.

^dRecovery attempted by reversing the rudder from full with to $\frac{2}{3}$ against the spin.

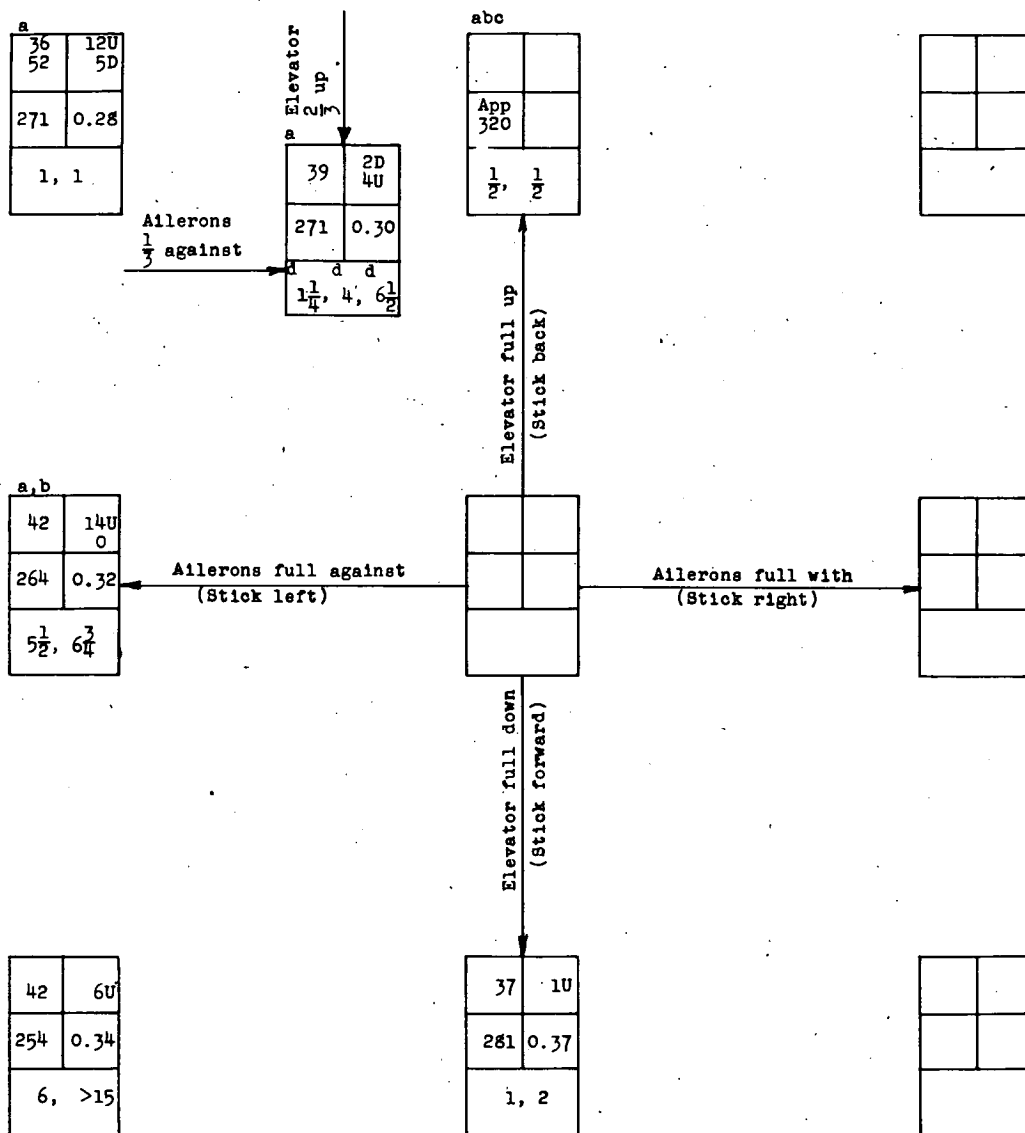
Model values converted to corresponding full-scale values.
U. inner wing up
D. inner wing down

α (deg)	ϕ (deg)
V (fps)	Ω (rps)
Turns for recovery	



CHART 5.- SPIN AND RECOVERY CHARACTERISTICS OF THE MODEL AT LOADING 2 AND
A TAIL-DAMPING POWER FACTOR OF 1557×10^{-6}

$$\left[\frac{I_x - I_y}{mb^2} = -394 \times 10^{-4}, \mu = 25, \text{ recovery attempted by rapid full rudder reversal unless otherwise noted, right spins} \right]$$



^aOscillatory in roll and yaw, average value or range of values given.

^bWandering spin.

^cRecovery attempted before model reached final attitude.

^dRecovery attempted by reversing the rudder from full with to $\frac{1}{3}$ against the spin.

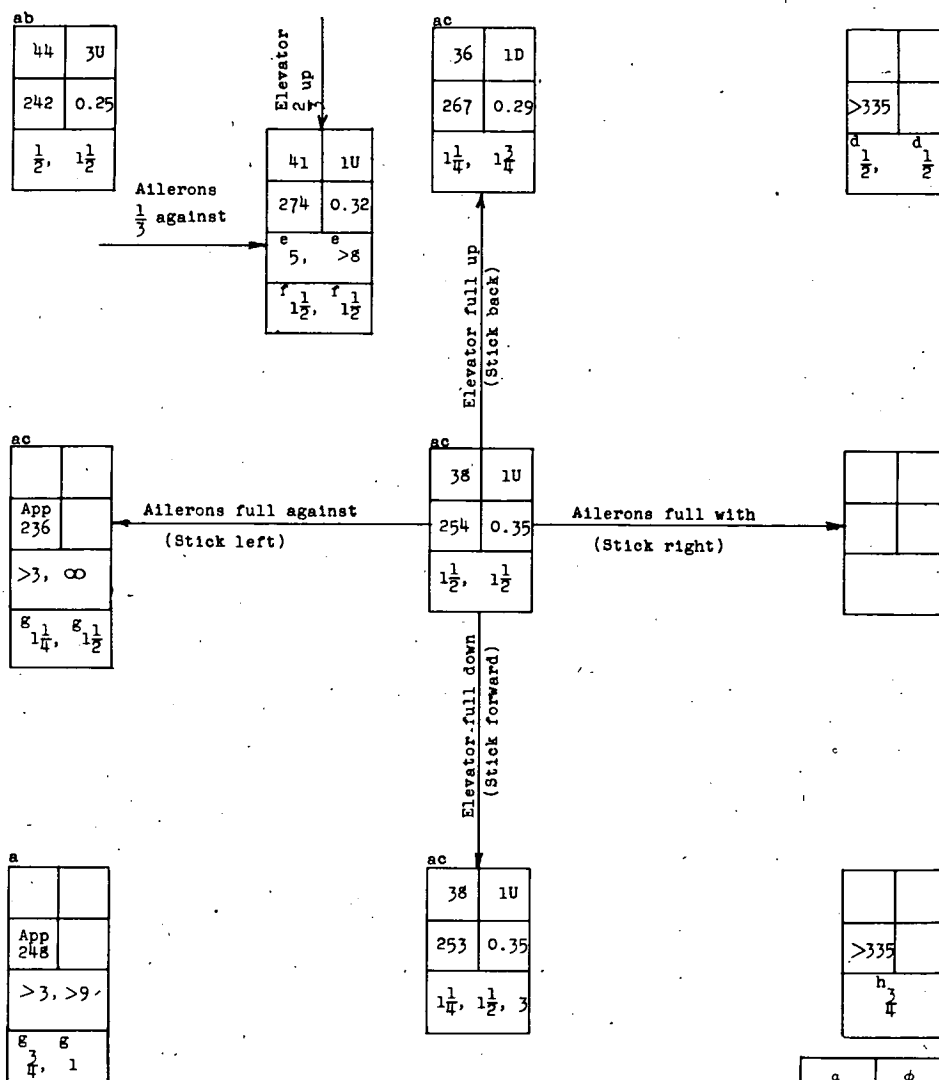
Model values converted to corresponding full-scale values.
U inner wing up
D inner wing down

a (deg)	φ (deg)
v (fps)	Ω (rps)
Turns for recovery	

NACA

CHART 6.- SPIN AND RECOVERY CHARACTERISTICS OF THE MODEL AT LOADING 2 AND
A TAIL-DAMPING POWER FACTOR OF 1079×10^{-6}

$$\left[\frac{I_x - I_y}{mb^2} = -394 \times 10^{-4}, \mu = 25, \text{recovery attempted by rapid full rudder reversal unless otherwise noted, right spins} \right]$$



^aWandering spin.

^bSpin oscillatory in yaw, roll, and pitch, average values given.

^cSlightly oscillatory, average values given.

^dRecovery attempted before model reached final attitude. Model recovered by going into an aileron roll.

^eRecovery attempted by reversing the rudder from full with to 2/3 against the spin.

^fRecovery attempted by simultaneous reversal of the ailerons from 1/3 against to full with the spin and the rudder from full with to 2/3 against the spin.

^gRecovery attempted by simultaneous full reversal of the ailerons to with the spin and the rudder to against the spin.

^hRecovery attempted before model in final attitude. Model recovered and went into an inverted spin.

Model values converted to corresponding full-scale values.
U inner wing up
D inner wing down

α (deg)	ϕ (deg)
V (fps)	Ω (rps)
Turns for recovery	

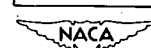
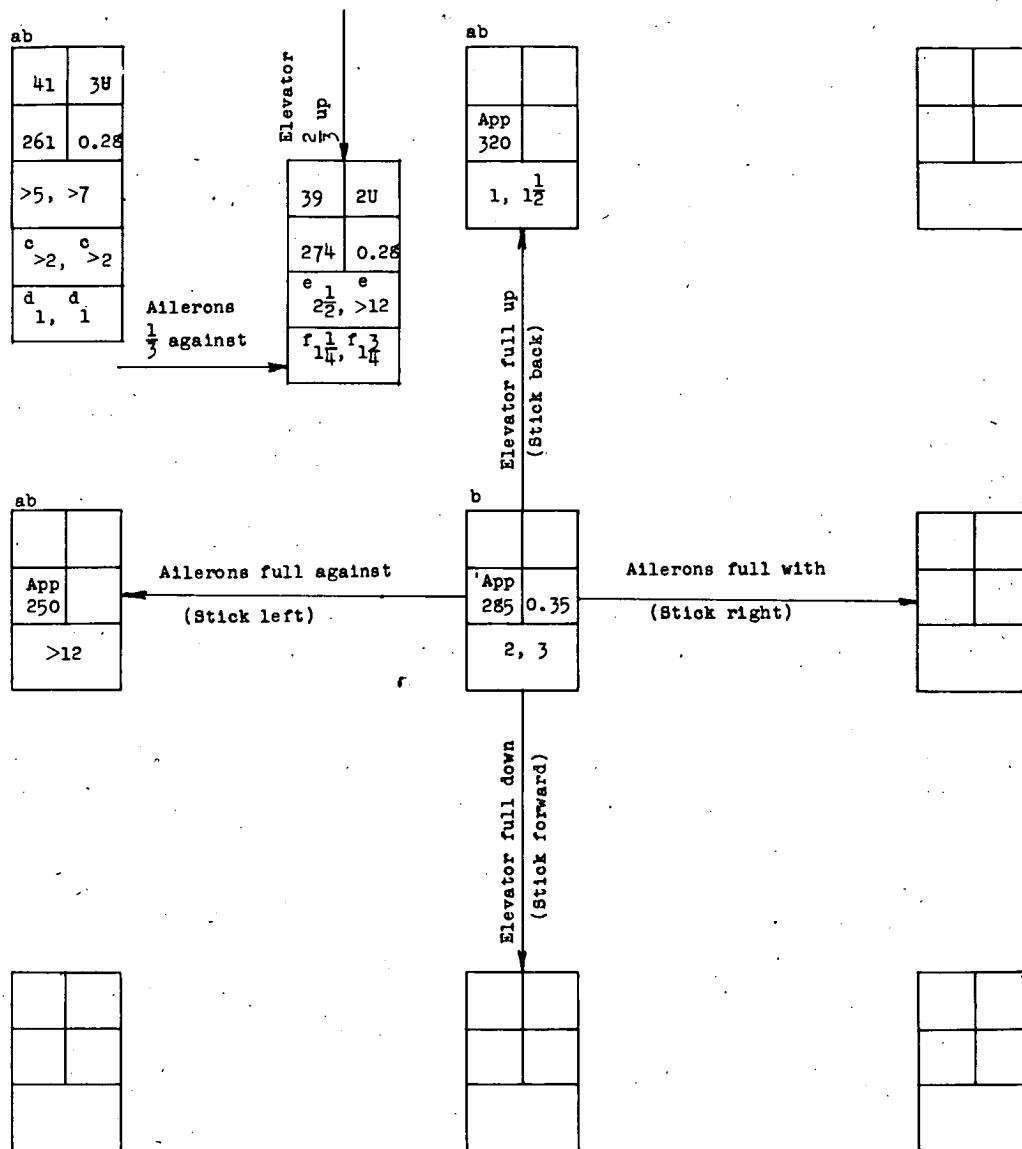


CHART 7.- SPIN AND RECOVERY CHARACTERISTICS OF THE MODEL AT LOADING 2 AND
A TAIL-DAMPING POWER FACTOR OF 0

$$\left[\frac{I_x - I_y}{mb^2} = -394 \times 10^{-4}, \mu = 25, \text{ recovery attempted by rapid full rudder reversal unless} \right. \\ \left. \text{otherwise noted, right spins} \right]$$



^aWhipping spin.

^bWandering spin.

^cRecovery attempted by full reversal of ailerons alone.

^dRecovery attempted by simultaneous full reversal of rudder and ailerons.

^eRecovery attempted by reversal of rudder from full with to $\frac{2}{3}$ against the spin.

^fRecovery attempted by simultaneous reversal of rudder from full with to $\frac{2}{3}$ against the spin and the ailerons from $\frac{1}{3}$ against to full with the spin.

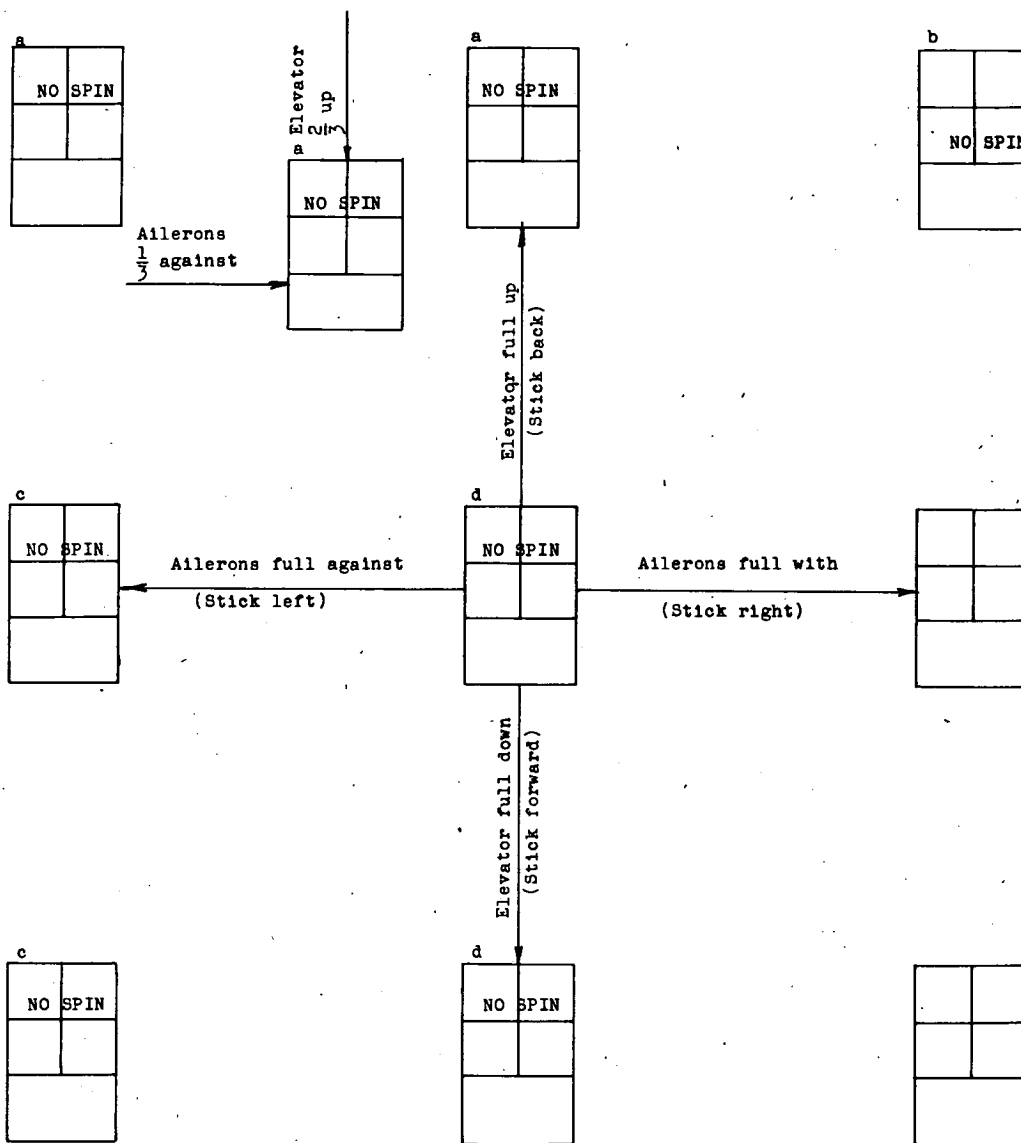
Model values converted to corresponding full-scale values.
U inner wing up
D inner wing down

α (deg)	ϕ (deg)
V (fps)	Ω (rps)
Turns for recovery	



CHART 8.- SPIN AND RECOVERY CHARACTERISTICS OF THE MODEL AT LOADING 3 AND
A TAIL-DAMPING POWER FACTOR OF 1079×10^{-6}

$$\left[\frac{I_x - I_y}{mb^2} = -671 \times 10^{-4}, \mu = 25, \text{right spins} \right]$$



^aAfter launching, the model motion became increasingly oscillatory in roll and yaw and the pitch angle decreased until the model abruptly went into an erect glide.

^bAfter launching, the model steepened until almost vertical and then went into an aileron roll.

^cAfter launching, the model motion became increasingly oscillatory in roll and yaw until the model rolled left, inverted, and continued in a left roll with the fuselage almost vertical.

^dAfter launching, the model motion became increasingly oscillatory in roll and yaw and the pitch angle decreased until the model abruptly went into an erect dive.

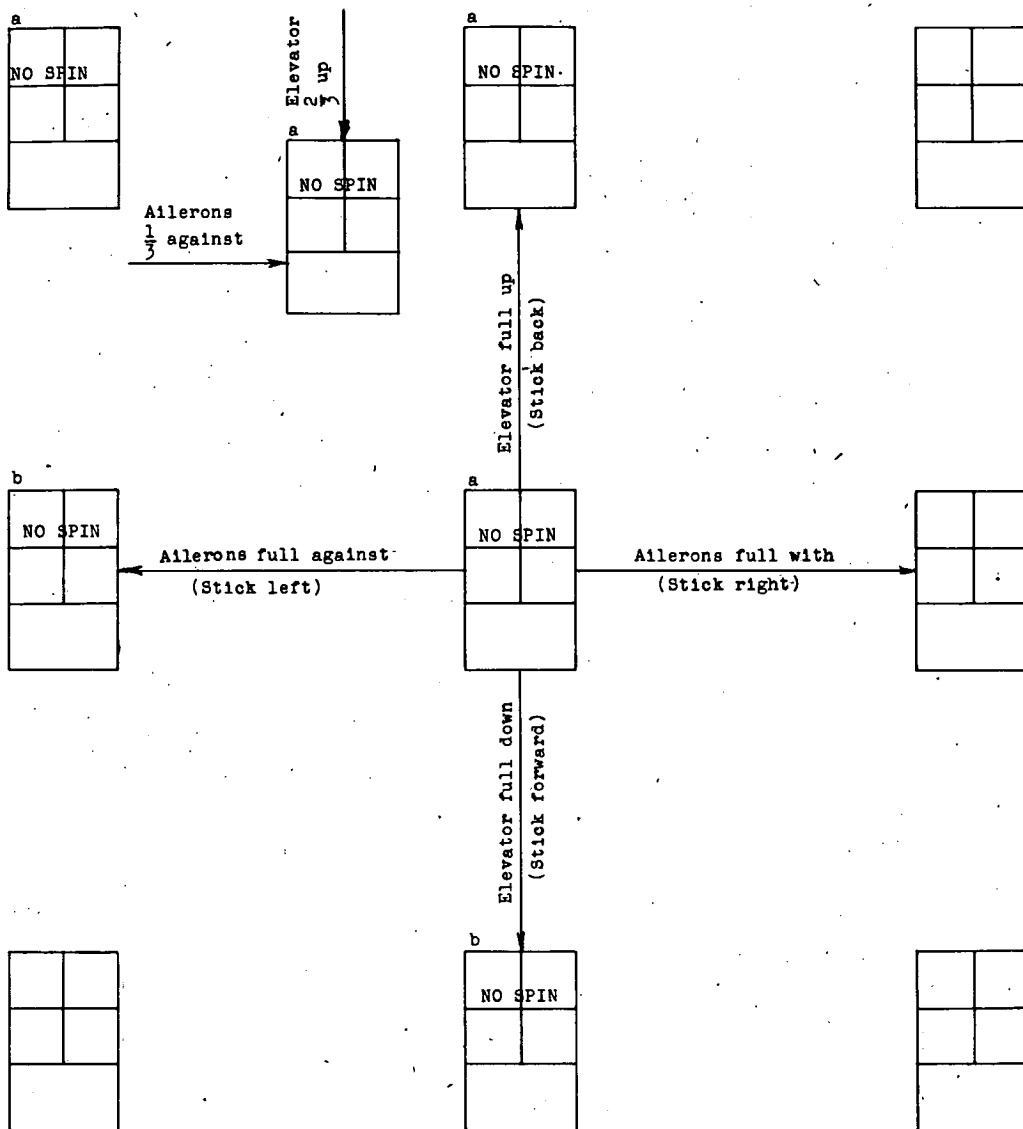
Model values
converted to
corresponding
full-scale values.
U inner wing up
D inner wing down

a (deg)	ϕ (deg)
V (fps)	Ω (rps)
Turns for recovery	



CHART 9.- SPIN AND RECOVERY CHARACTERISTICS OF THE MODEL AT LOADING 3
AND A TAIL-DAMPING POWER FACTOR OF 0

$$\left[\frac{I_X - I_Y}{mb^2} = -671 \times 10^{-4}, \mu = 25, \text{right spins} \right]$$



^a After launching, the model motion became increasingly oscillatory in roll and yaw and the pitch angle decreased until the model abruptly went into an erect dive.

^b After launching, the model motion became increasingly oscillatory in roll and yaw until the model rolled left, inverted, and continued in a left roll with the fuselage almost vertical.

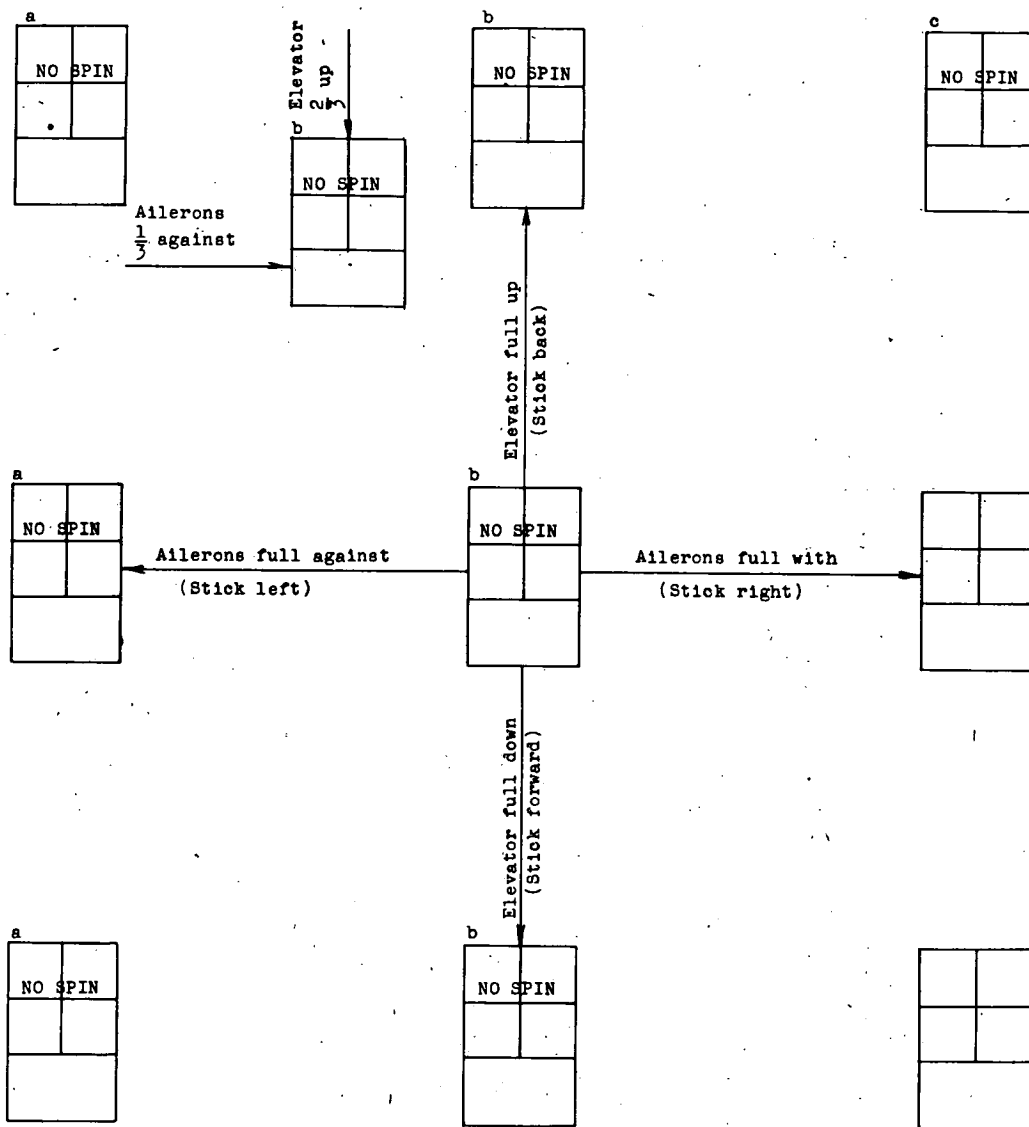
Model values converted to corresponding full-scale values.
U inner wing up
D inner wing down

α (deg)	ϕ (deg)
V (fps)	Ω (rps)
Turns for recovery	



CHART 10.- SPIN AND RECOVERY CHARACTERISTICS OF THE MODEL AT LOADING 4
AND A TAIL-DAMPING POWER FACTOR OF 1079×10^{-6}

$$\left[\frac{I_X - I_Y}{mb^2} = -865 \times 10^{-4}, \mu = 25, \text{right spins} \right]$$



^aAfter launching, the model motion became increasingly oscillatory in roll and yaw until the model rolled left, inverted, and continued in a left roll with the fuselage almost vertical.

^bAfter launching, the model motion was slightly oscillatory in roll and yaw and the pitch angle decreased until the model abruptly went into an erect dive.

^cAfter launching, the model steepened until almost vertical and then went into an aileron roll.

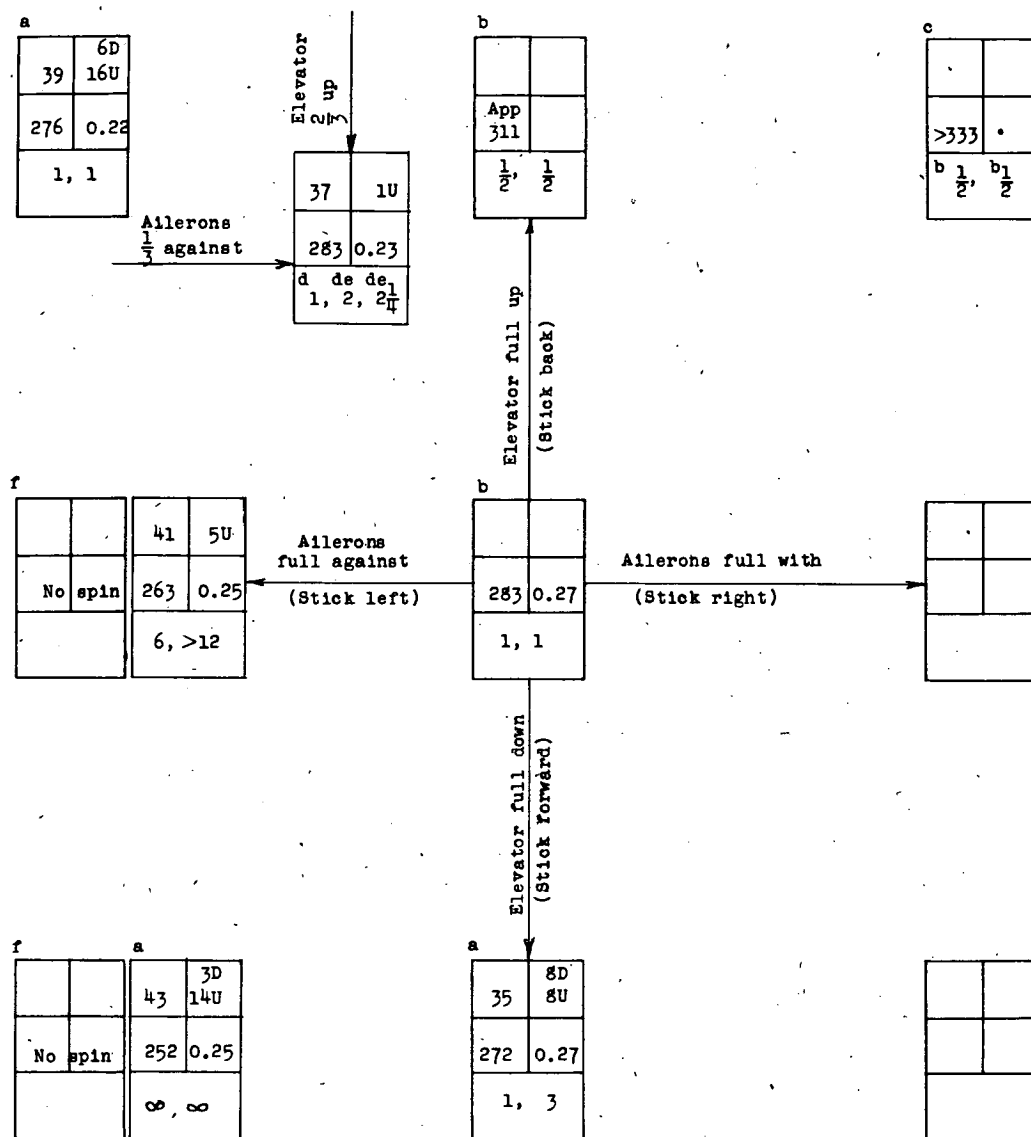
Model values
converted to
corresponding
full-scale values.
U inner wing up
D inner wing down

α (deg)	ϕ (deg)
V (fps)	Ω (rps)
Turns for recovery	

NACA

CHART 11.- SPIN AND RECOVERY CHARACTERISTICS OF THE MODEL AT LOADING 5
AND A TAIL-DAMPING POWER FACTOR OF 2020×10^{-6}

$\frac{I_x - I_y}{mb^2} = -1052 \times 10^{-4}$, $\mu = 25$, recovery attempted by rapid full rudder reversal unless otherwise noted, right spins]



^aOscillatory spin. Average value or range of values given.

^bWandering spin.

^cRecovery attempted before model in final steeper attitude. Model recovered by going into an aileron roll.

^dRecovery attempted by reversing the rudder from full with to $\frac{2}{3}$ against the spin.

^eVisual observation.

^fAfter launching, the model motion became increasingly oscillatory in roll and yaw until the model rolled left, inverted, and continued in a left roll with the fuselage almost vertical.

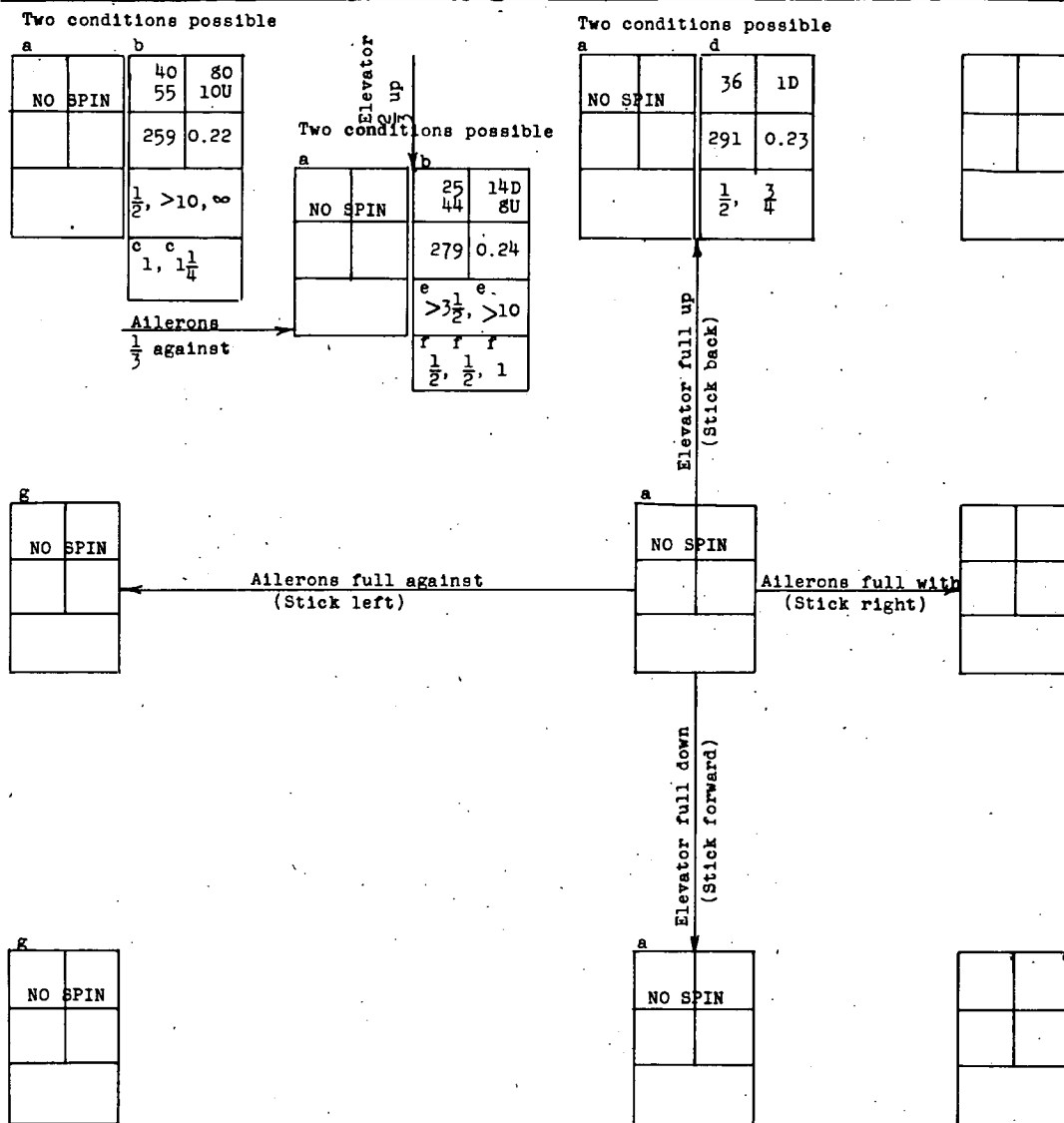
Model values converted to corresponding full-scale values.
U inner wing up
D inner wing down

α (deg)	ϕ (deg)
V (fps)	Ω (rps)
Turns for recovery	

NACA

CHART 14.- SPIN AND RECOVERY CHARACTERISTICS OF THE MODEL AT LOADING 5
AND A TAIL-DAMPING POWER FACTOR OF 0

$$\left[\frac{I_x - I_y}{mb^2} = -1052 \times 10^{-4}, \mu = 25, \text{ recovery attempted by rapid full rudder reversal unless otherwise noted, right spins} \right]$$



^aAfter launching, the model motion became increasingly oscillatory in roll and yaw, and the pitch angle decreased until the model abruptly went into erect dive.

^bOscillatory spin, range of values or average value given.

^cRecovery attempted by simultaneous full reversal of the ailerons to with the spin and the rudder to against the spin.

^dWhipping spin.

^eRecovery attempted by reversing the rudder from full with to $\frac{2}{3}$ against the spin:

^fRecovery attempted by simultaneous reversal of the rudder from full with to $\frac{2}{3}$ against the spin and the ailerons from $\frac{1}{2}$ against to full with the spin.

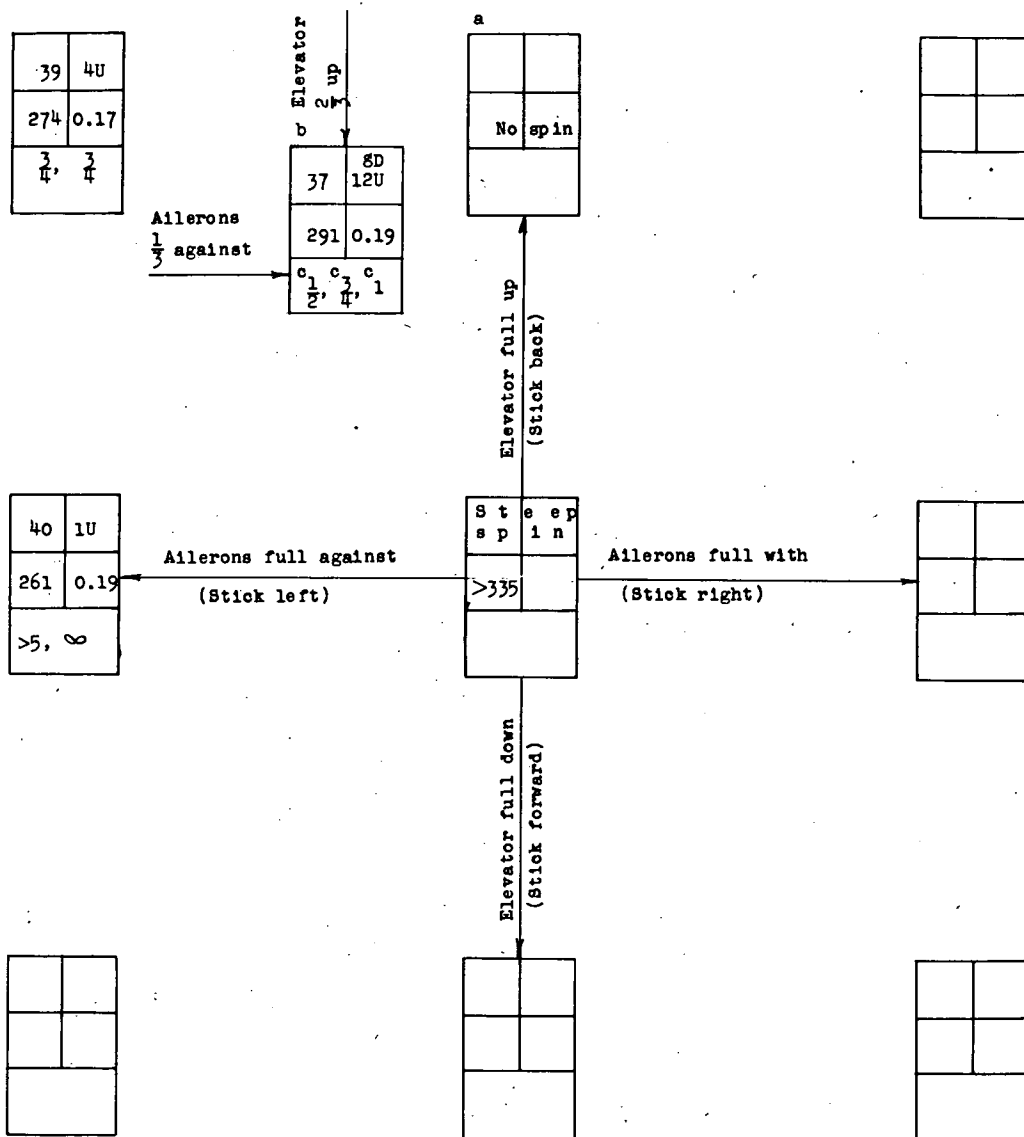
^gAfter launching, the model motion became increasingly oscillatory in roll and yaw until the model rolled left, inverted, and continued in a left roll with the fuselage almost vertical.

Model values converted to corresponding full-scale values.
U inner wing up
D inner wing down

α (deg)	ϕ (deg)
V (fps)	Ω (rps)
Turns for recovery	

CHART 15.- SPIN AND RECOVERY CHARACTERISTICS OF THE MODEL, AT LOADING 6
AND A TAIL-DAMPING POWER FACTOR OF 2020×10^{-6}

$$\left[\frac{I_x - I_y}{mb^2} = -1571 \times 10^{-4}, \mu = 25, \text{recovery attempted by rapid full rudder reversal unless otherwise noted, right spins} \right]$$



^aAfter launching, the model motion was slightly oscillatory in roll and yaw, and the pitch angle decreased until the model abruptly went into an erect dive.

^bOscillatory spin, average value or range of values given.

^cRecovery attempted by reversing the rudder from full with to $\frac{2}{3}$ against the spin.

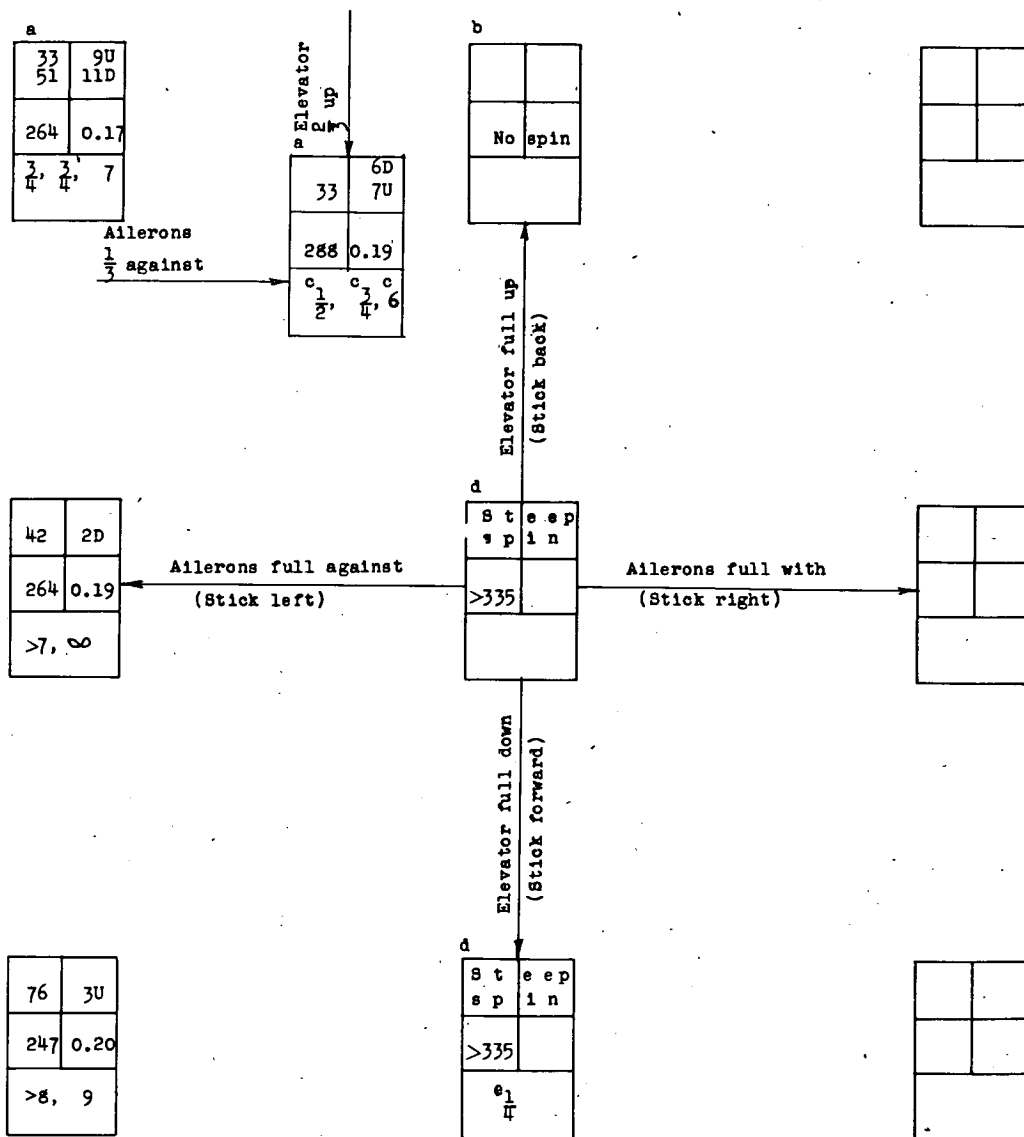
Model values converted to corresponding full-scale values.
U inner wing up
D inner wing down

a (deg)	ϕ (deg)
v (fps)	Ω (rps)
Turns for recovery	



CHART 16.- SPIN AND RECOVERY CHARACTERISTICS OF THE MODEL AT LOADING 6
AND A TAIL-DAMPING POWER FACTOR OF 1557×10^{-6}

$$\left[\frac{I_X - I_Y}{mb^2} = -1571 \times 10^{-4}, \mu = 25, \text{ recovery attempted by rapid full rudder reversal unless otherwise noted, right spins} \right]$$



^aWandering and oscillatory spin. Average value or range of values given.

^bAfter launching, the model motion was slightly oscillatory in roll and yaw and the pitch angle decreased until the model abruptly went into an erect dive.

^cRecovery attempted by reversing the rudder from full with to $\frac{2}{3}$ against the spin.

^dRecovery attempted before model reached its final steep attitude.

^eModel recovers in an inverted dive.

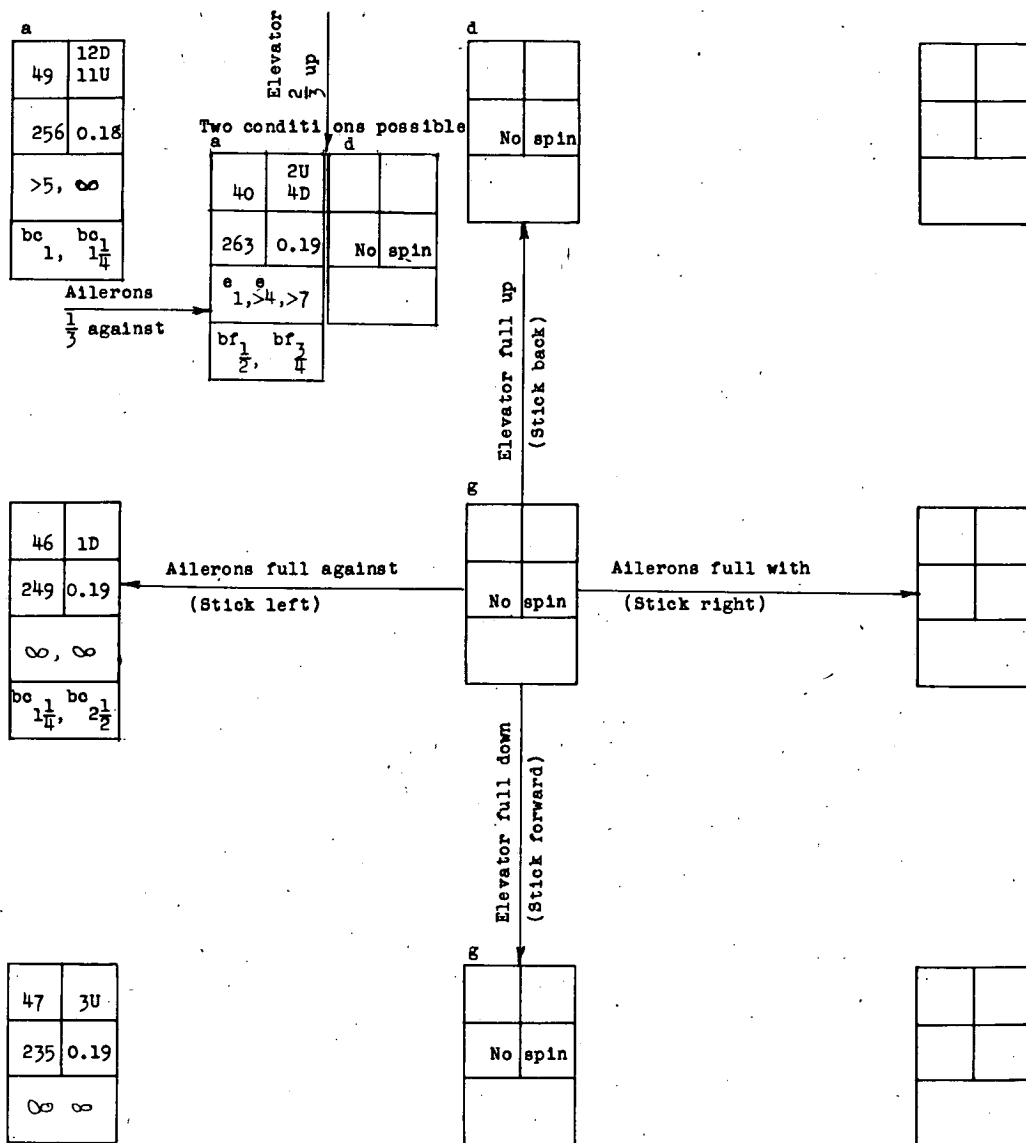
Model values converted to corresponding full-scale values.
U inner wing up
D inner wing down

α (deg)	ϕ (deg)
V (fps)	Ω (rps)
Turns for recovery	

NACA

CHART 17.- SPIN AND RECOVERY CHARACTERISTICS OF THE MODEL AT LOADING 6
AND A TAIL-DAMPING POWER FACTOR OF 1079×10^{-6}

$$\left[\frac{I_x - I_y}{mb^2} = -1571 \times 10^{-4}, \mu = 25, \text{recovery attempted by rapid full rudder reversal unless otherwise noted, right spins} \right]$$



^a Spin oscillatory in roll and yaw. Average value or range of values given.

^b Visual observation..

^c Recovery attempted by simultaneous full reversal of the ailerons to with the spin and the rudder to against the spin.

^d After launching the model spins with increasing radius until it goes into an erect glide.

^e Recovery attempted by reversing the rudder from full with to $\frac{2}{3}$ against the spin.

^f Recovery attempted by simultaneous reversal of ailerons from $\frac{1}{3}$ against the spin to full with the spin and the rudder from full with to $\frac{2}{3}$ against the spin.

^g After launching, the model motion became increasingly oscillatory in roll and yaw and the pitch angle decreased until the model abruptly went into an erect dive.

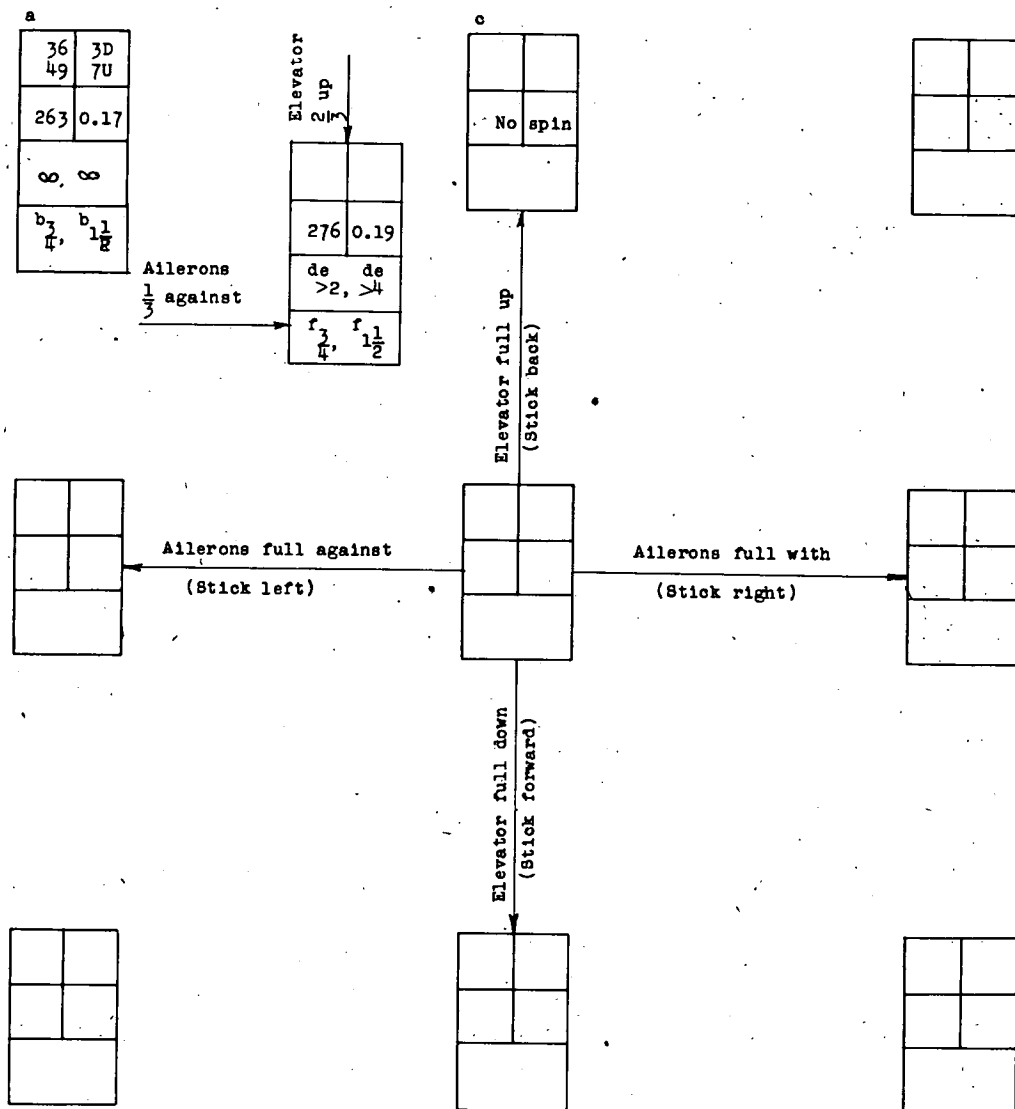
Model values converted to corresponding full-scale values.
U inner wing up
D inner wing down

a (deg)	φ (deg)
V (fps)	Ω (rps)
Turns for recovery	

NACA

CHART 18.- SPIN AND RECOVERY CHARACTERISTICS OF THE MODEL AT LOADING 6
AND A TAIL-DAMPING POWER FACTOR OF 0

$$\left[\frac{I_x - I_y}{mb^2} = -1571 \times 10^{-4}, \mu = 25, \text{ recovery attempted by rapid full rudder reversal unless otherwise noted, right spins} \right]$$



^a Oscillatory spin. Average value or range of values given.

^b Recovery attempted by simultaneous full reversal of the ailerons to with the spin and the rudder to against the spin.

^c After launching, the model motion was slightly oscillatory in roll and yaw and the pitch angle decreased until the model abruptly went into an erect dive.

^d Recovery attempted by reversing the rudder from full with to $\frac{2}{3}$ against the spin.

^e Visual observation.

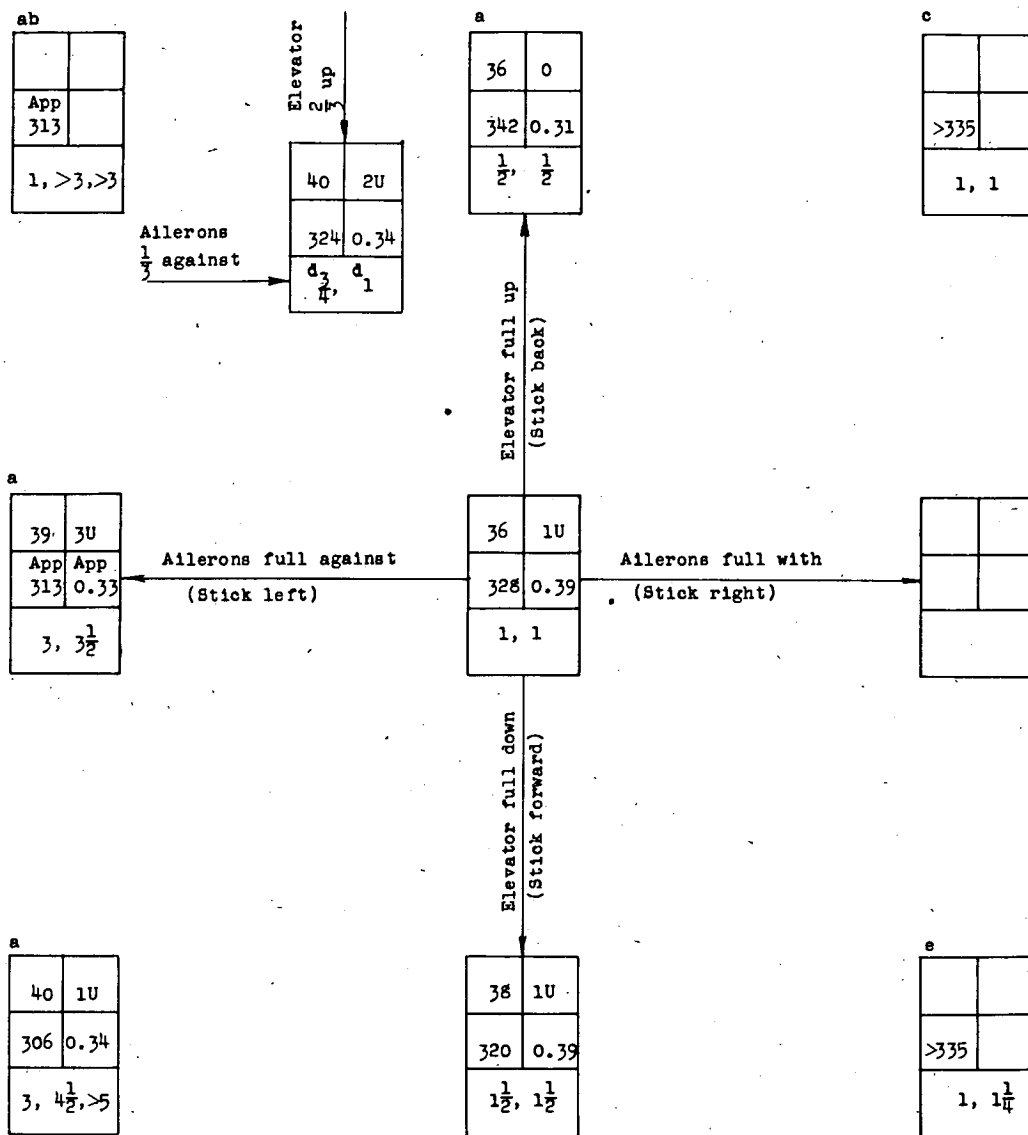
^f Recovery attempted by simultaneous reversal of the rudder from full with to $\frac{2}{3}$ against the spin and the ailerons from $\frac{1}{3}$ against to full with the spin.

NACA

CHART 19.- SPIN AND RECOVERY CHARACTERISTICS OF THE MODEL AT LOADING 7

AND A TAIL-DAMPING POWER FACTOR OF 1079×10^{-6}

$\frac{I_x - I_y}{mb^2} = -208 \times 10^{-4}$, $\mu = 35$, recovery attempted by rapid full rudder reversal unless otherwise noted, right spins]

^aWandering spin.^bWhipping spin.^cRecovery attempted before model in final attitude. Model recovered by going into an aileron roll.^dRecovery attempted by reversing rudder from full with to $\frac{2}{3}$ against the spin.^eRecovery attempted before model in final attitude. Model recovered and then went into an inverted spin.

Model values converted to corresponding full-scale values.
 U inner wing up
 D inner wing down

α (deg)	ϕ (deg)
V (fps)	Ω (rps)
Turns for recovery	

NACA

CHART 20.- SPIN AND RECOVERY CHARACTERISTICS OF THE MODEL AT LOADING 8
AND A TAIL-DAMPING POWER FACTOR OF 1079×10^{-6}

$\frac{I_x - I_y}{mb^2} = -425 \times 10^{-4}$, $\mu = 35$, recovery attempted by rapid full rudder reversal unless otherwise noted, right spins]

Two conditions possible

a

>335	
$\frac{1}{2}$, $\frac{1}{2}$, >3	>5

Ailerons
 $\frac{1}{3}$ against

Elevator
 $\frac{2}{3}$ up

e

No spin	

Ailerons full against
(Stick left)

Two conditions possible

b

No spin	
$\frac{1}{2}$	

Elevator full up
(Stick back)

App	278
$\frac{1}{2}$, $\frac{1}{4}$	

Elevator full down
(Stick forward)

App	278
$\frac{3}{4}$, 1	

Ailerons full with
(Stick right)

>335	
$\frac{1}{2}$, $\frac{3}{4}$	

>335	
$\frac{1}{2}$, $\frac{1}{2}$	

a Wandering, oscillatory spin. Recovery attempted before model in final attitude.

b After launching model, the model motion became slightly oscillatory in roll and yaw and the pitch angle decreased until the model abruptly went into an erect dive.

c Recovery attempted by reversing rudder from full with to $\frac{1}{3}$ against the spin.

d Recovery attempted before model in final attitude. Model recovered by going into an aileron roll.

e After launching model becomes increasingly oscillatory in roll and yaw until model rolled left, inverted, and continued into a left roll with the fuselage almost vertical.

f Recovery attempted before model in final attitude. Model recovered and then went into an inverted spin.

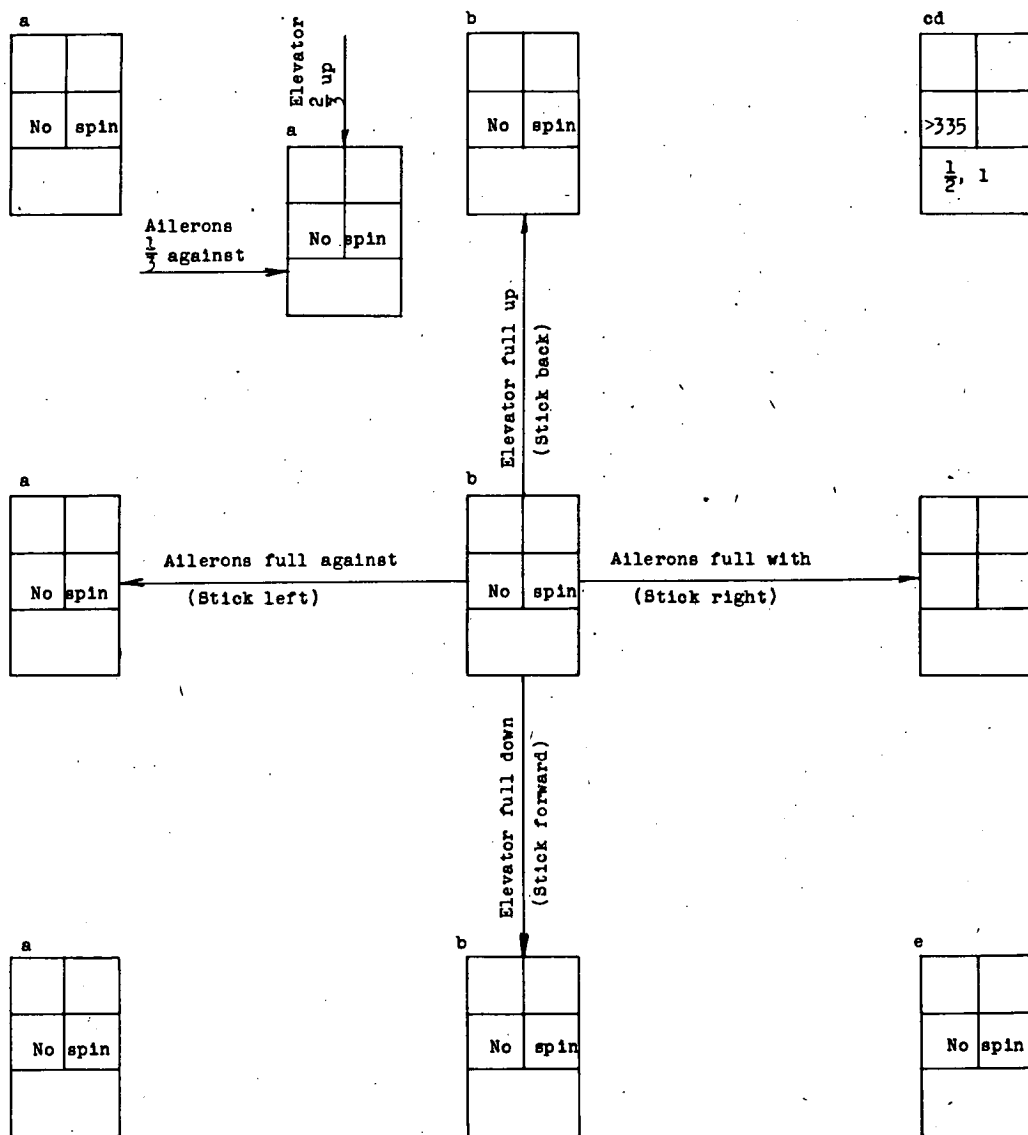
Model values converted to corresponding full-scale values.
U: inner wing up.
D: inner wing down

a (deg)	ϕ (deg)
v (fps)	Ω (rps)
Turns for recovery	



CHART 21.- SPIN AND RECOVERY CHARACTERISTICS OF THE MODEL AT LOADING 9
AND A TAIL-DAMPING POWER FACTOR OF 1079×10^{-6}

$$\frac{I_x - I_y}{mb^2} = -627 \times 10^{-4}, \mu = 35, \text{ recovery attempted by rapid full rudder reversal unless otherwise noted, right spins }]$$



^a After launching, the model motion became increasingly oscillatory in roll and yaw until the model rolled left, inverted, and continued into a left roll with the fuselage almost vertical.

^b After launching, the model motion was slightly oscillatory in roll and yaw and the pitch angle decreased until the model abruptly went into an erect dive.

^c Recovery attempted before model reached its final steep attitude.

^d Whipping spin. Might be no spin if model could have been held longer.

^e After launching, the model steepened and increased its radius until it went into a spiral glide.

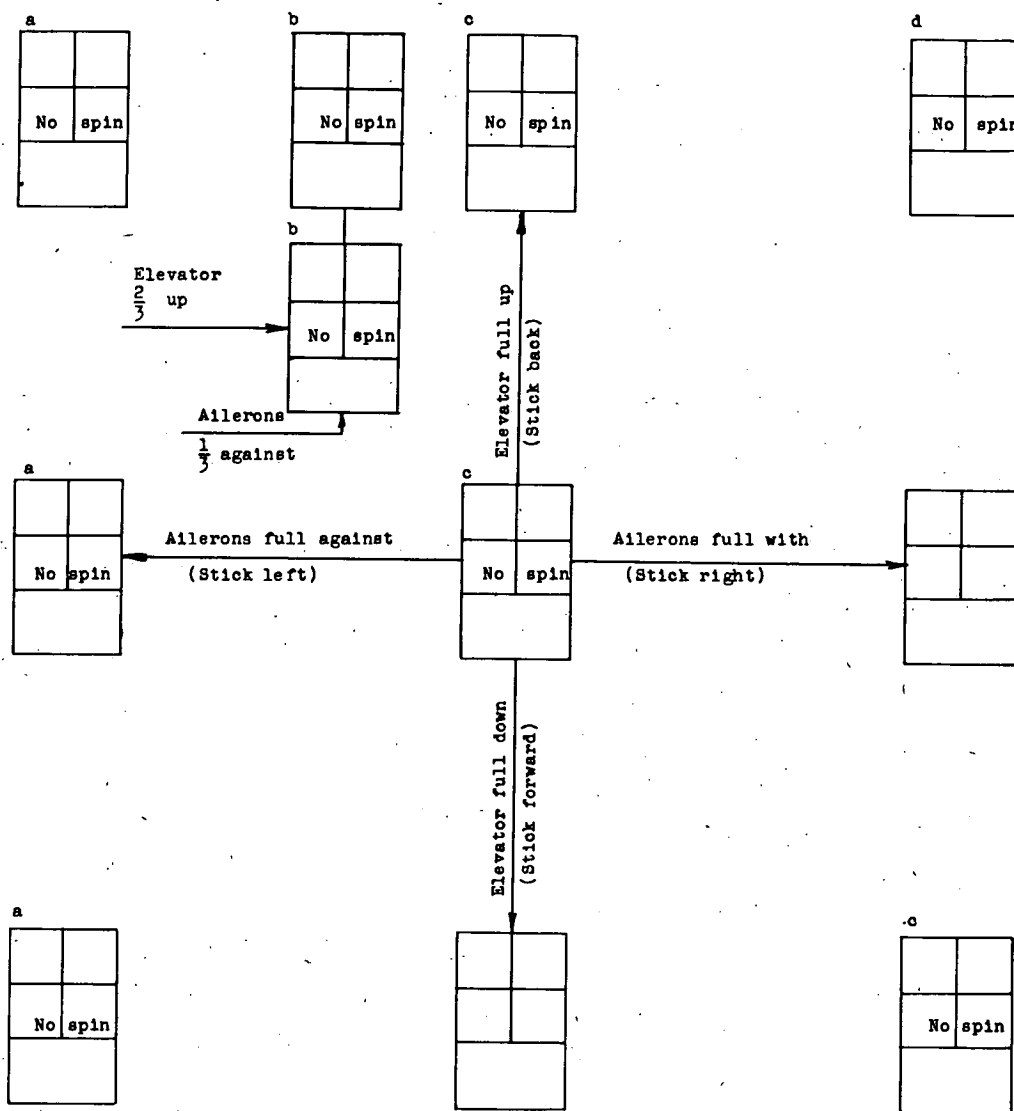
Model values converted to corresponding full-scale values.
U inner wing up
D inner wing down

α (deg)	ϕ (deg)
V (fps)	Ω (rps)
Turns for recovery	

NACA

CHART 22.- SPIN AND RECOVERY CHARACTERISTICS OF THE MODEL AT LOADING 10
AND A TAIL-DAMPING POWER FACTOR OF 0

$$\left[\frac{I_x - I_y}{mb^2} = -843 \times 10^{-4}, \mu = 35, \text{ recovery attempted by rapid full rudder reversal unless otherwise noted, right spins} \right]$$



^a After launching, the model became increasingly oscillatory in roll and yaw until the model rolled left, inverted, and continued in a left roll with the fuselage almost vertical.

^b After launching the model started oscillating mainly in roll. The amplitude of the roll increased until a roll of about 60° (inner wing up) occurred and the model then pitched to a very steep angle of attack and dived vertically approximately 15 feet. The wings leveled out, the nose came up, and the model then smoothly entered a right spin again.

^c After launching, the model motion was slightly oscillatory in roll and yaw and the pitch angle decreased until the model abruptly went into an erect dive.

^d After launching, the model steepened and increased its radius until it went into a spiral glide.

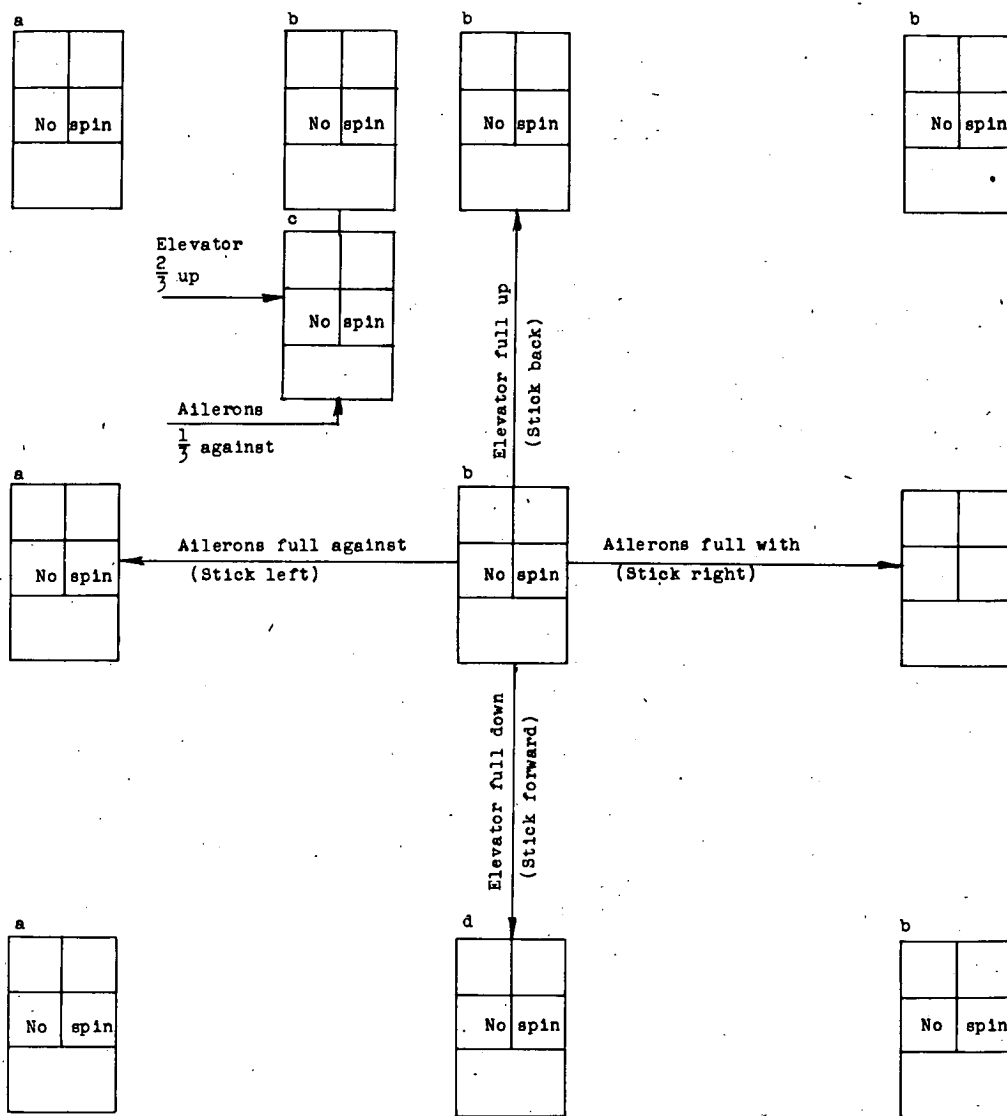
Model values
converted to
corresponding
full-scale values.
U inner wing up
D inner wing down

α (deg)	ϕ (deg)
V (fps)	Ω (rps)
Turns for recovery	

NACA

CHART 23.- SPIN AND RECOVERY CHARACTERISTICS OF THE MODEL AT LOADING 10
AND A TAIL-DAMPING POWER FACTOR OF 1079×10^{-6}

$\frac{I_x - I_y}{mb^2} = -843 \times 10^{-4}$, $\mu = 35$, recovery attempted by rapid full rudder reversal unless otherwise noted, right spins]



^a After launching, the model became increasingly oscillatory in roll and yaw until the model rolled left, inverted, and continued in a left roll with the fuselage almost vertical.

^b After launching, the model motion was slightly oscillatory in roll and yaw, and the pitch angle decreased until the model abruptly went into a dive.

^c After launching, the model started oscillating mainly in roll. The amplitude of the roll increased until a roll of about 60° (inner wing up) occurred and the model then pitched to a very steep angle of attack and dived vertically approximately 15 feet. The wings leveled out, the nose came up, and the model then smoothly entered a right spin again.

^d After launching, the model motion was slightly oscillatory in roll and yaw and the pitch angle decreased until the model abruptly went into an inverted dive.

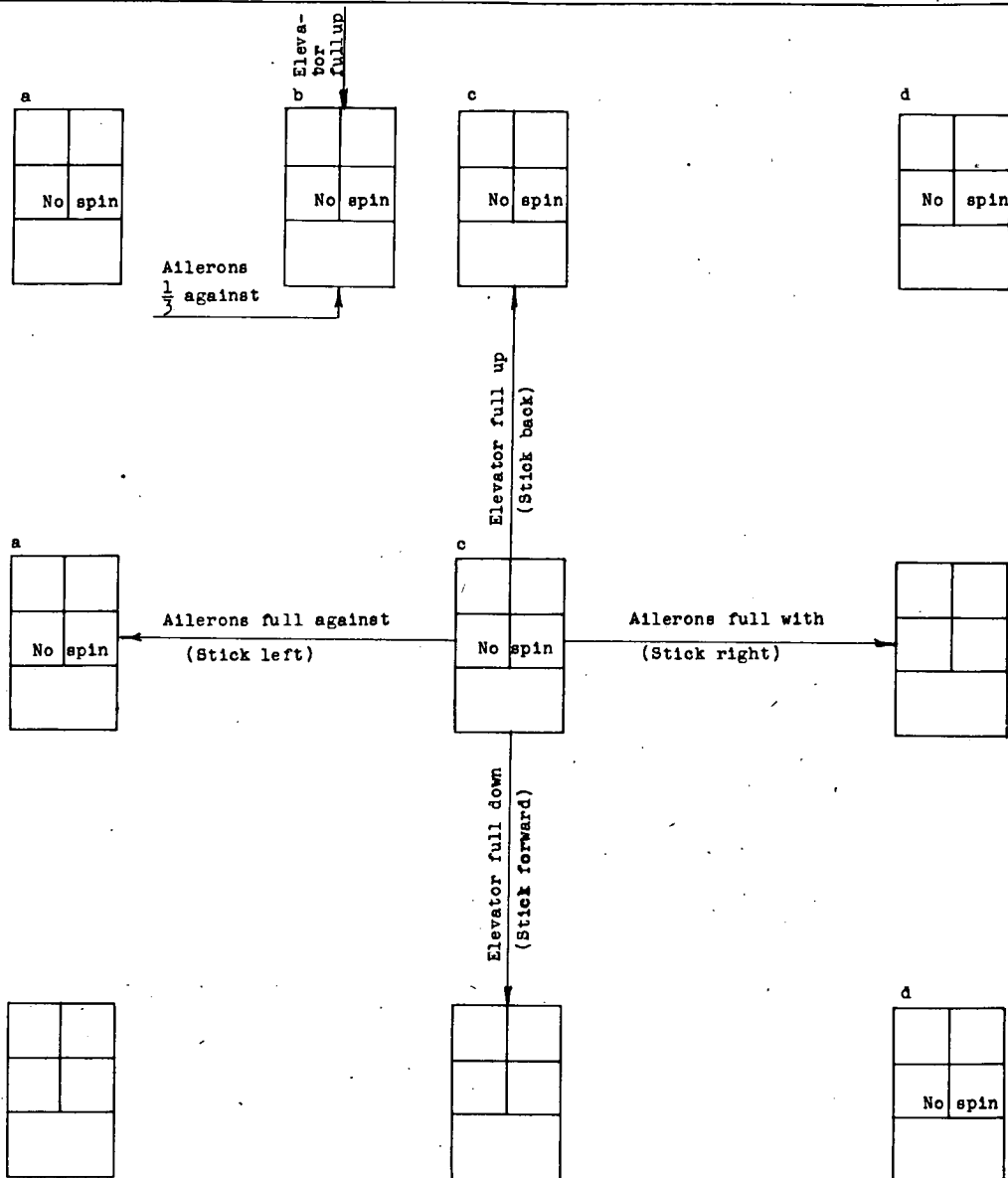
Model values converted to corresponding full-scale values.
U inner wing up
D inner wing down

α (deg)	ϕ (deg)
V (fps)	Ω (rps)
Turns for recovery	



CHART 24.- SPIN AND RECOVERY CHARACTERISTICS OF THE MODEL AT LOADING 10
AND A TAIL-DAMPING POWER FACTOR OF 1557×10^{-6}

$$\left[\frac{I_x - I_y}{mb^2} = -843 \times 10^{-4}, \mu = 35, \text{ recovery attempted by rapid full rudder reversal unless otherwise noted, right spins} \right]$$



^a After launching, the model became increasingly oscillatory in roll and yaw until the model rolled left, inverted, and continued in a left roll with the fuselage almost vertical.

^b After launching, the model started oscillating mainly in roll. The amplitude of the roll increased until a roll of about 60° (inner wing up) occurred and the model then pitched to a very steep angle of attack and dived vertically approximately 15 feet. The wings leveled out, the nose came up, and the model then smoothly entered a right spin again.

^c After launching, the model motion was slightly oscillatory in roll and yaw and the pitch angle decreased until the model abruptly went into an erect dive.

^d After launching, the model steepened until almost vertical and then went into an aileron roll.

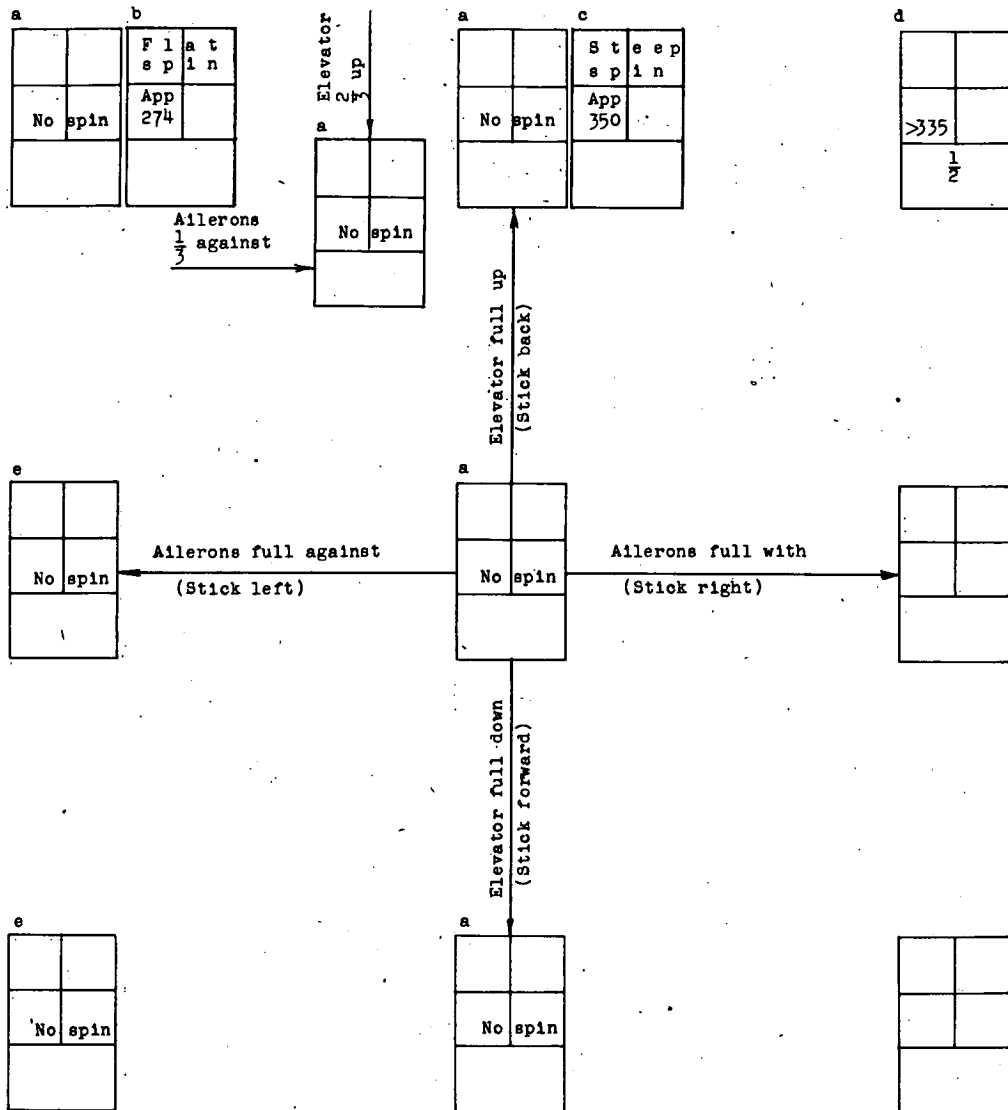
Model values converted to corresponding full-scale values.
U inner wing up
D inner wing down

α (deg)	ϕ (deg)
V (fps)	Ω (rps)
Turns for recovery	



CHART 25.- SPIN AND RECOVERY CHARACTERISTICS OF THE MODEL AT LOADING 11
AND A TAIL-DAMPING POWER FACTOR OF 0

$\frac{I_x - I_y}{mb^2} = -997 \times 10^{-4}$, $\mu = 35$, recovery attempted by rapid full rudder reversal unless otherwise noted, right spins]



^aAfter launching, the model motion was slightly oscillatory in roll and yaw and the pitch angle decreased until the model abruptly went into an erect dive.

^bSpin oscillatory in roll and yaw, pitch remaining fairly constant. Recoveries would probably be unsatisfactory.

^cOscillatory and wandering spin. Might be no spin if model could have been held longer.

^dRecovery attempted before model in final attitude. Model recovered by going into an aileron roll.

^eAfter launching, model becomes increasingly oscillatory in roll, pitch, and yaw until model rolled left, inverted, and continued in a left roll with the fuselage almost vertical.

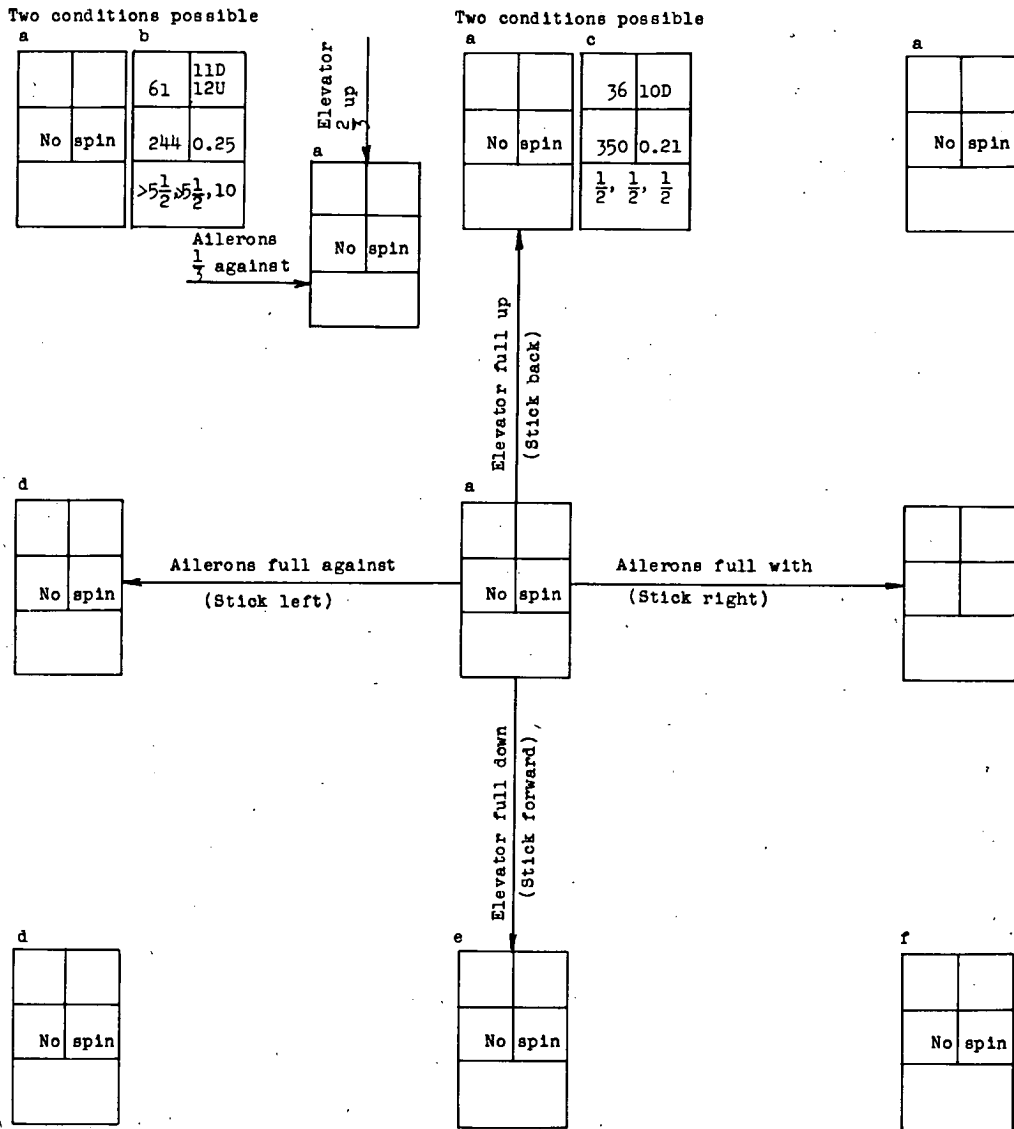
Model values converted to corresponding full-scale values.
U inner wing up
D inner wing down

a (deg)	φ (deg)
v (fps)	Ω (rps)
Turns for recovery	



CHART 26.- SPIN AND RECOVERY CHARACTERISTICS OF THE MODEL AT LOADING 11
AND A TAIL-DAMPING POWER FACTOR OF 1079×10^{-6}

$$\left[\frac{I_x - I_y}{mb^2} = -997 \times 10^{-4}, \mu = 35, \text{ recovery attempted by rapid full rudder reversal unless otherwise noted, right spins} \right]$$



^aAfter launching, the model motion was slightly oscillatory in roll and yaw and the pitch angle decreased until the model abruptly went into an erect dive.

^bOscillatory spin, average value or range of values given.

^cWandering spin with periodic whip.

^dAfter launching, the model became increasingly oscillatory in roll and yaw until the model rolled left, inverted, and continued in a left roll with the fuselage almost vertical.

^eAfter launching, the model motion was slightly oscillatory in roll and yaw and the pitch angle decreased until the model abruptly went into an inverted dive.

^fAfter launching, the model attitude steepened until model dived vertically out of the spin.

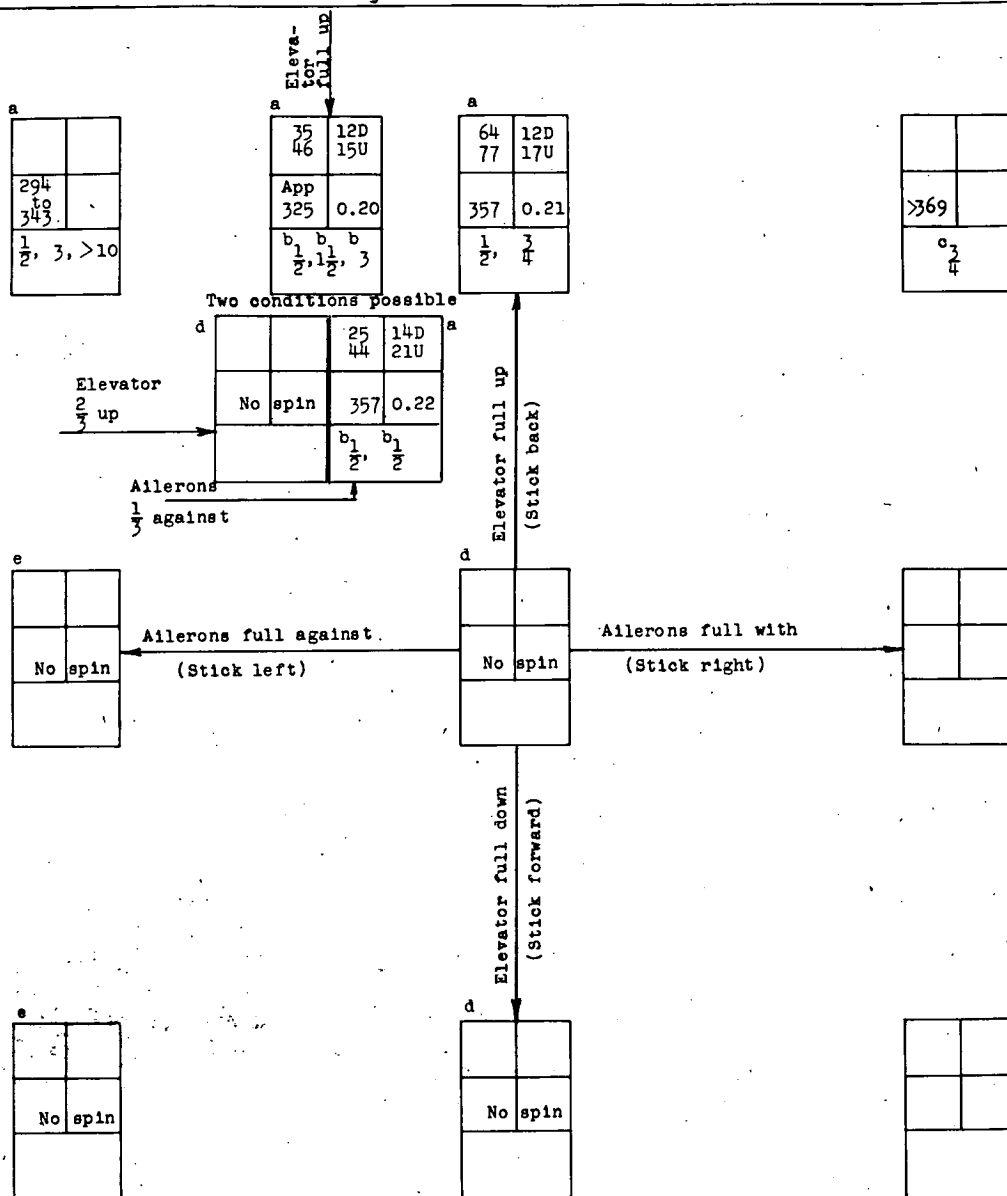
Model values converted to corresponding full-scale values.
U inner wing up
D inner wing down

a (deg)	φ (deg)
v (fps)	Ω (rps)
Turns for recovery	

NACA

CHART 27.- SPIN AND RECOVERY CHARACTERISTICS OF THE MODEL AT LOADING 11
AND A TAIL-DAMPING POWER FACTOR OF 1557×10^{-6}

$$\left[\frac{I_x - I_y}{mb^2} = -997 \times 10^{-4}, \mu = 35, \text{ recovery attempted by rapid full rudder reversal unless otherwise noted, right spins} \right]$$



^aWandering and oscillatory spin, average value or range of values given.
^bRecovery attempted by reversal of the rudder from full with to $\frac{2}{3}$ against the spin.

^cRecovery attempted before model reached its final steep attitude. Model recovered by going into an aileron roll.

^dAfter launching, the model motion was slightly oscillatory in roll and yaw and the pitch angle decreased until the model abruptly went into an erect dive.

^eAfter launching, the model became increasingly oscillatory in roll and yaw until the model rolled left, inverted, and continued in a left roll with the fuselage almost vertical.

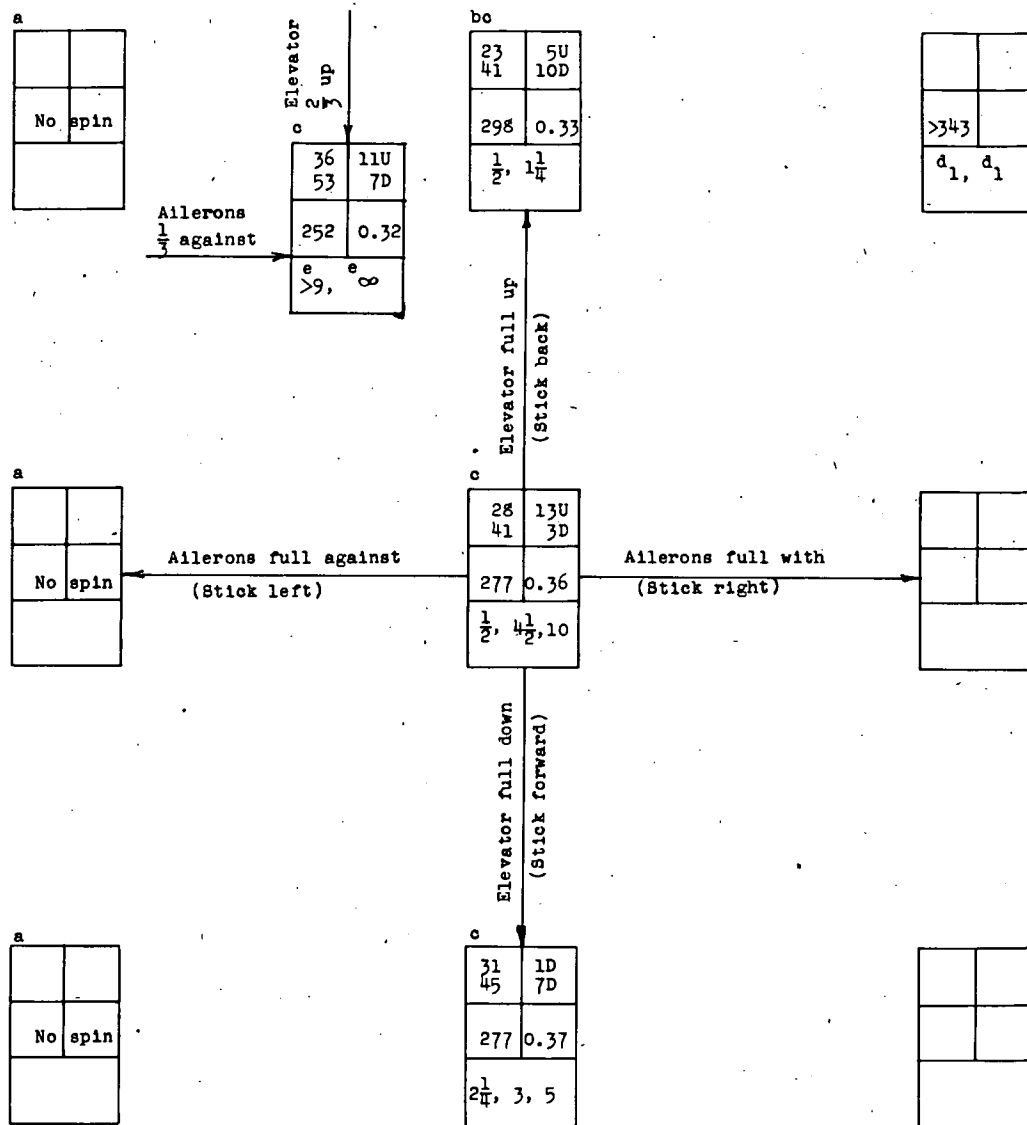
Model values converted to corresponding full-scale values.
U inner wing up
D inner wing down

α (deg)	ϕ (deg)
V (fps)	Ω (rps)
Turns for recovery	

NACA

CHART 28.- SPIN AND RECOVERY CHARACTERISTICS OF THE MODEL AT LOADING 12 WITH THE CENTER-OF-GRAVITY LOCATION AT 11 PERCENT \bar{c} AND A TAIL-DAMPING POWER FACTOR OF 1079×10^{-6}

$$\left[\frac{I_x - I_y}{mb^2} = -615 \times 10^{-4}, \mu = 25, \text{ recovery attempted by rapid full rudder reversal unless otherwise noted, right spins} \right]$$



^aAfter launching the model motion became increasingly oscillatory in roll and yaw and the pitch angle decreased until the model abruptly went into an erect dive.

^bWandering spin.

^cOscillatory spin, average value or range of values given.

^dRecovery attempted before model in final attitude. Model recovered by going into an aileron roll.

^eRecovery attempted by reversing rudder from full with to $\frac{2}{3}$ against the spin.

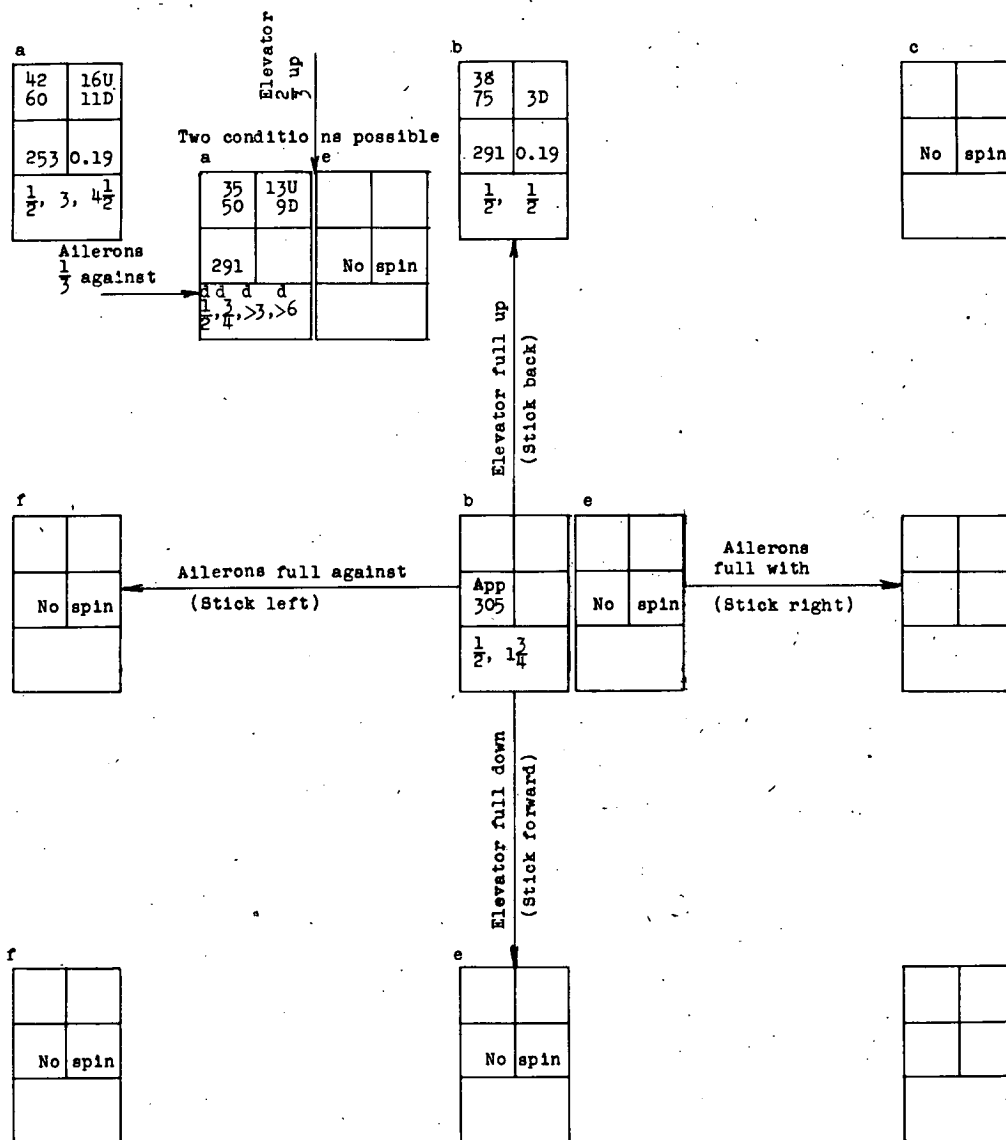
Model values converted to corresponding full-scale values.
U inner wing up
D inner wing down

α (deg)	ϕ (deg)
V (fps)	Ω (rps)
Turns for recovery	



CHART 29.- SPIN AND RECOVERY CHARACTERISTICS OF THE MODEL AT LOADING 13 WITH THE CENTER-OF-GRAVITY LOCATION AT 39 PERCENT \bar{c} AND A TAIL-DAMPING POWER FACTOR OF 1079×10^{-6}

$$\left[\frac{I_x - I_y}{mb^2} = -605 \times 10^{-4}, \mu = 25, \text{ recovery attempted by rapid full rudder reversal unless otherwise noted, right spins} \right]$$



^aSpin oscillatory in roll, yaw, and pitch. Average value or range of values given.

^bWandering, whipping spin.

^cModel spin radius increased until the model went into an erect glide.

^dRecovery attempted by reversal of the rudder from full with to $\frac{1}{3}$ against the spin.

^eAfter launching, the model motion became increasingly oscillatory in roll and yaw and the pitch angle decreased until the model abruptly went into a dive.

^fAfter launching, the model motion became increasingly oscillatory in roll and yaw until the model rolled left, inverted, and continued in a left roll with the fuselage almost vertical.

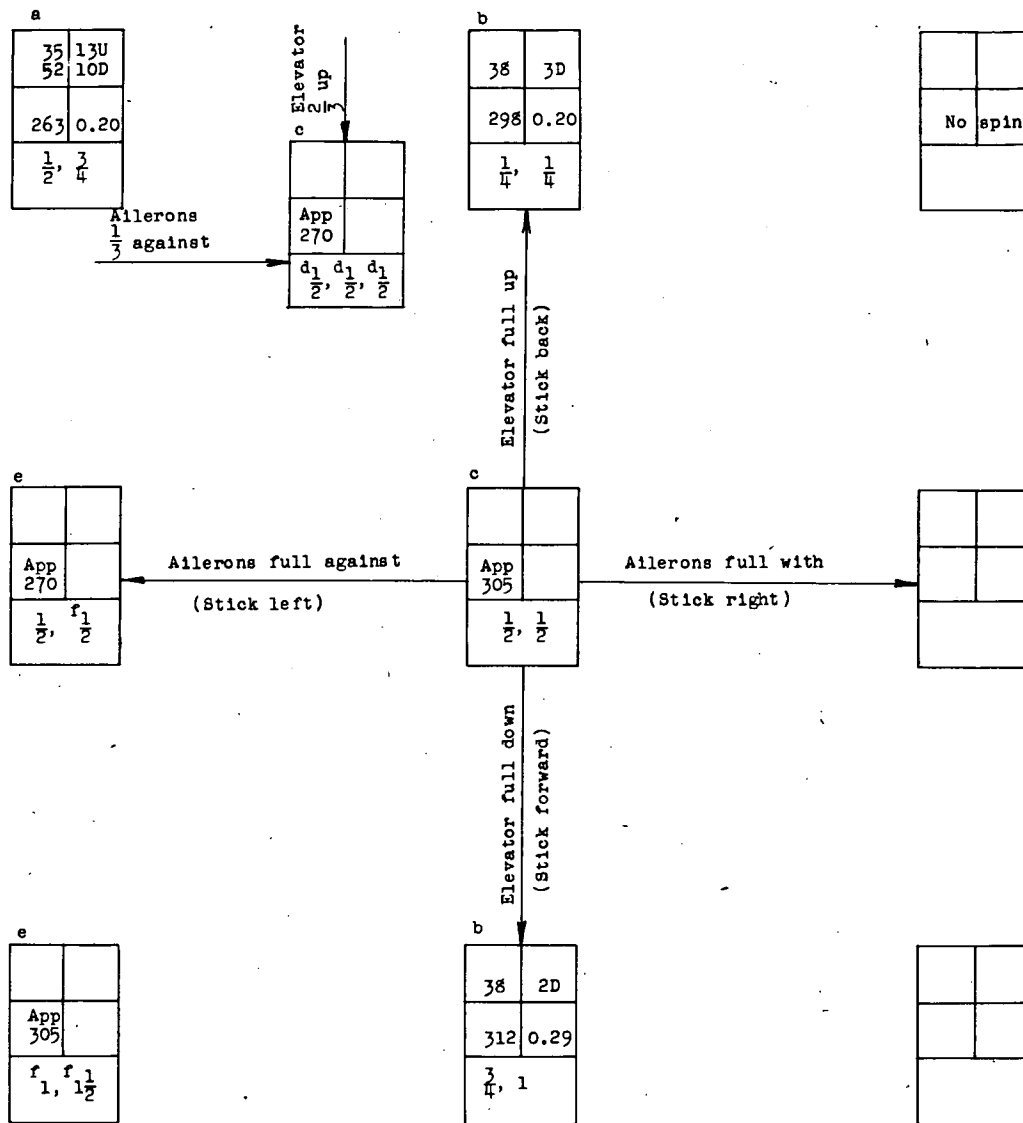
Model values converted to corresponding full-scale values.
U inner wing up
D inner wing down

α (deg)	ϕ (deg)
V (fps)	Ω (rps)
Turns for recovery	

NACA

CHART 30.- SPIN AND RECOVERY CHARACTERISTICS OF THE MODEL AT LOADING 14 WITH THE CENTER-OF-GRAVITY LOCATION AT 39 PERCENT \bar{c} AND A TAIL-DAMPING POWER FACTOR OF 1079×10^{-6}

$\left[\frac{I_x - I_y}{mb^2} = -162 \times 10^{-4}, \mu = 25, \text{ recovery attempted by rapid full rudder reversal unless otherwise noted, right spins} \right]$



^aWandering and oscillatory spin. Average value or range of values given.

^bWandering spin.

^cSpin so wandering that steady-spin data could not be obtained.

^dRecovery attempted by reversing the rudder from full with to $\frac{2}{3}$ against the spin.

^eWandering and oscillatory spin. Steady-spin data could not be obtained.

^fVisual observation.

Model values converted to corresponding full-scale values.
U inner wing up
D inner wing down

a	ϕ
(deg)	(deg)
v	Ω
(fps)	(rps)
Turns for recovery	



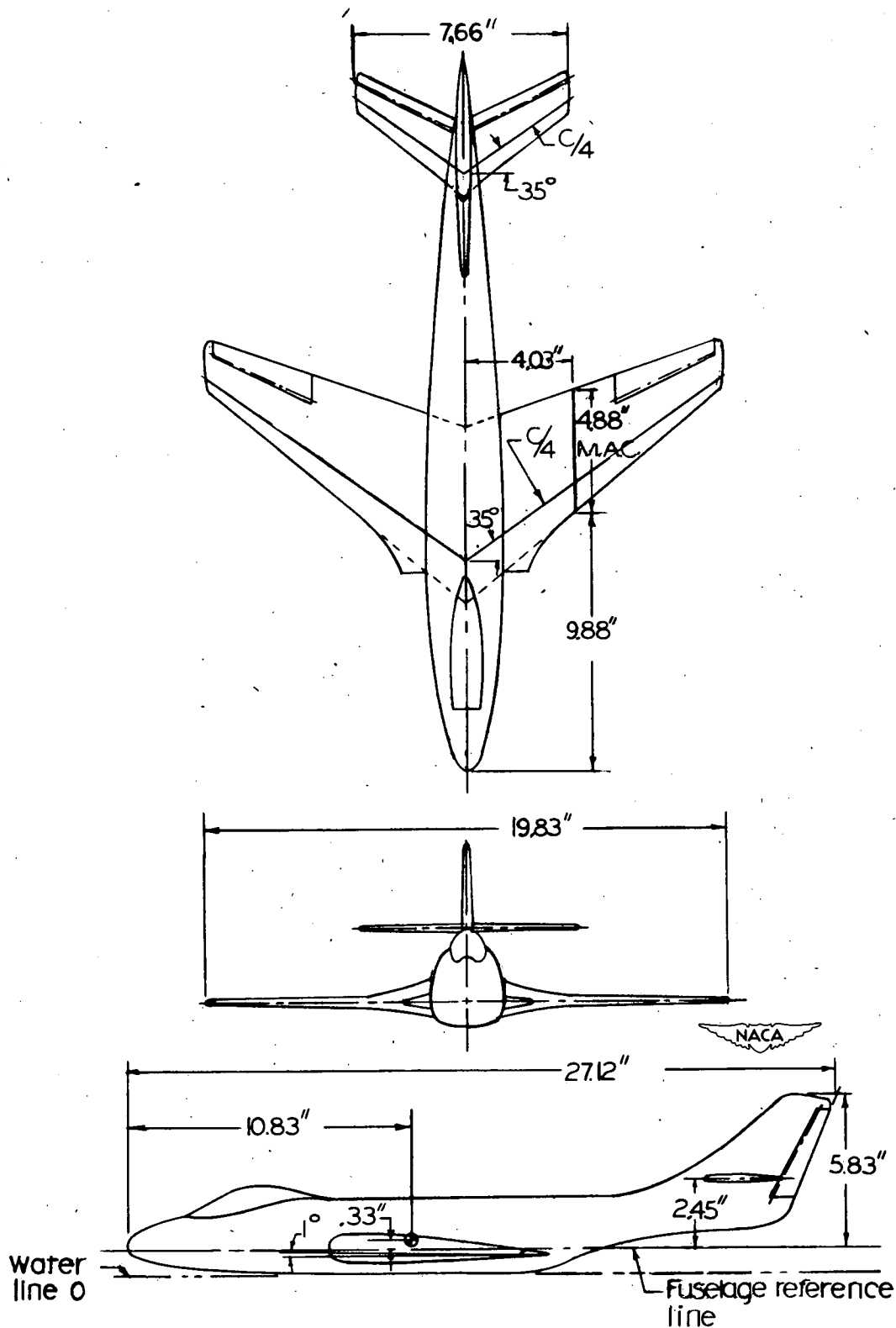


Figure 1.- Three-view drawing of the model of a swept-wing airplane investigated.

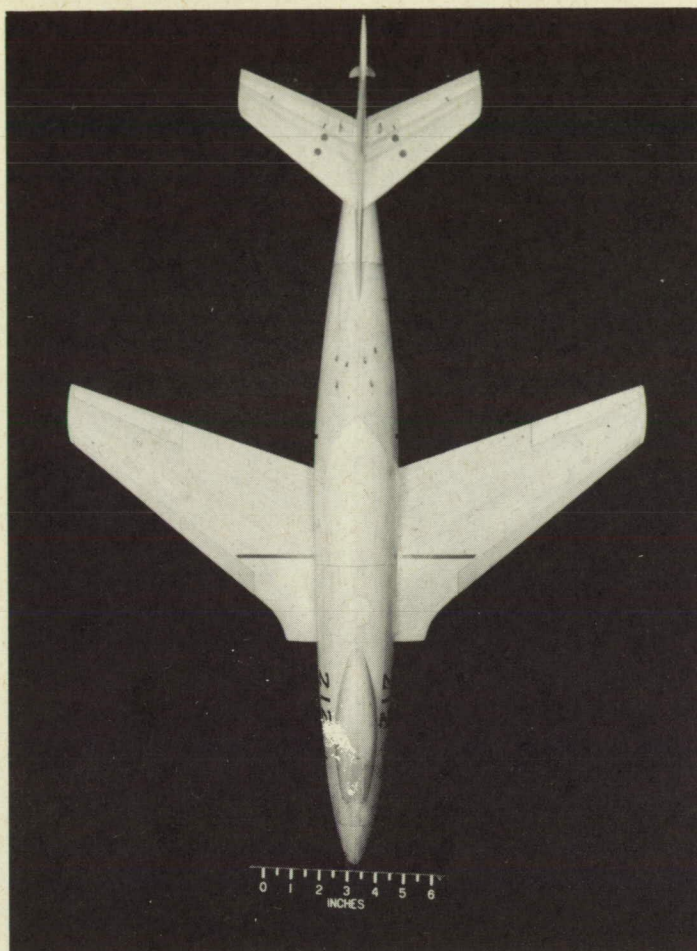


Figure 2.- Photographs of the model of a swept-wing airplane.

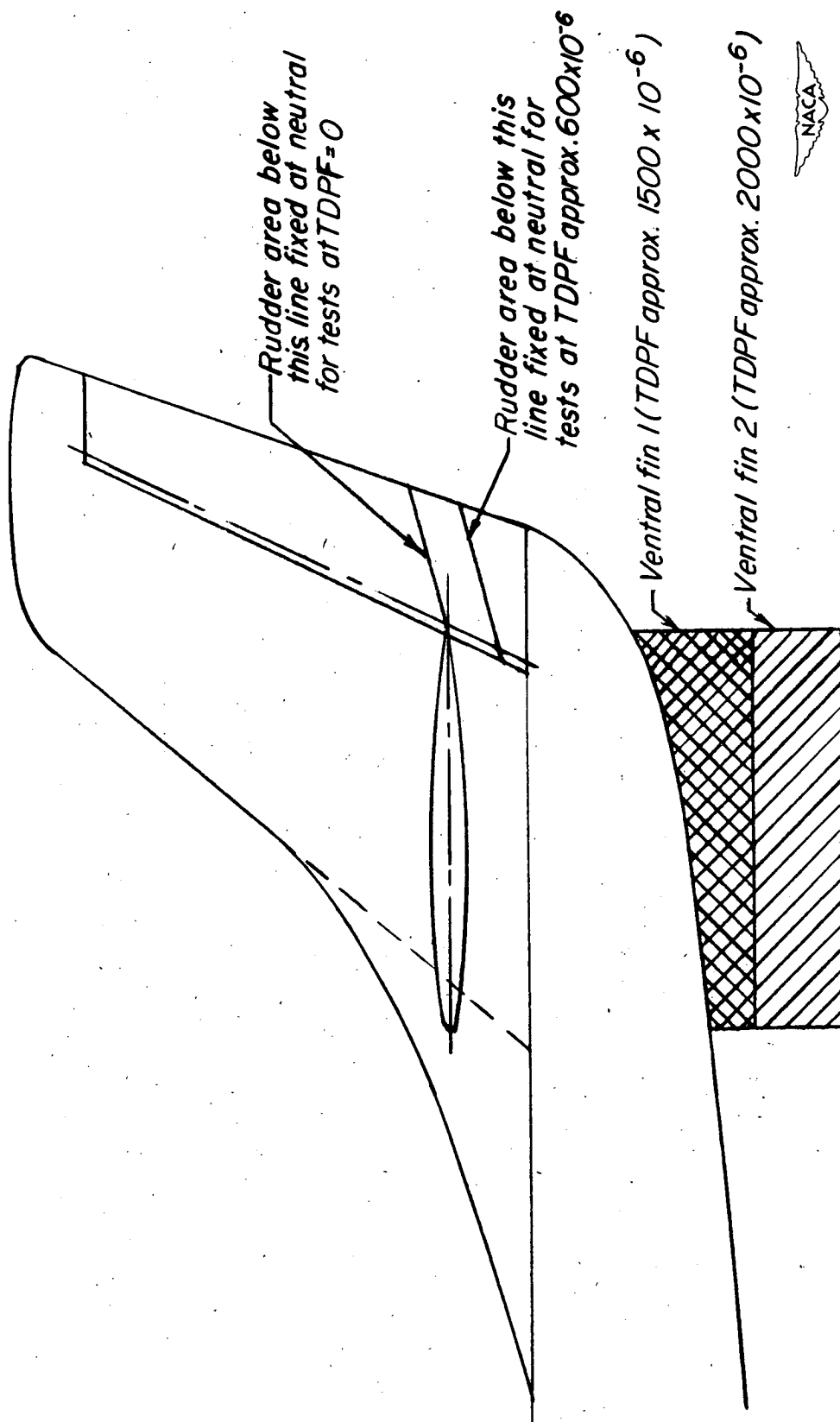


Figure 3.- Modifications by means of which tail-damping power factor was changed on the model. For normal tail with no ventral fins and entire rudder movable, tail-damping power factor approximately 1000×10^{-6} .



Figure 4.- Photograph of the model of a swept-wing airplane spinning in the Langley 20-foot free-spinning tunnel.

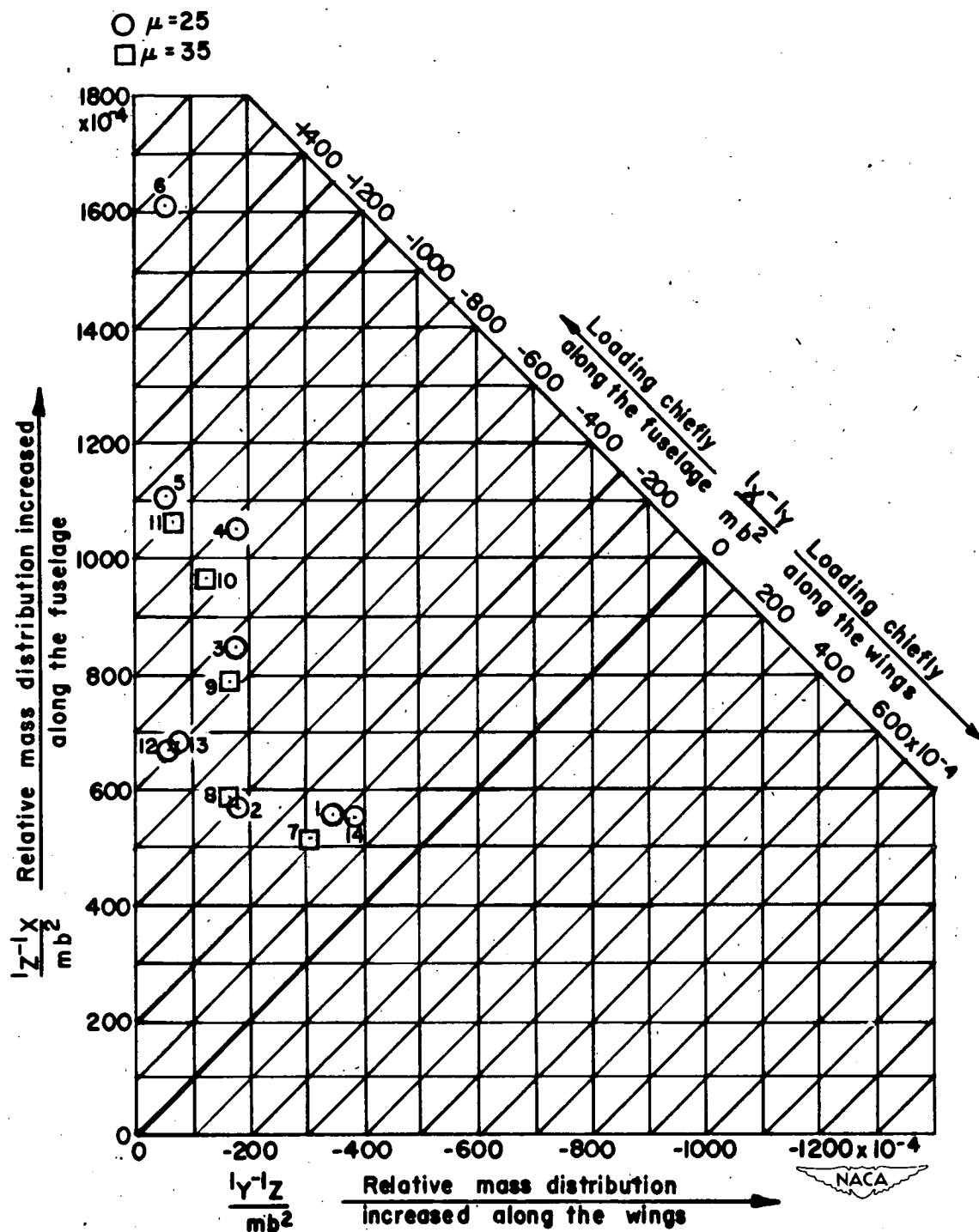


Figure 5.- Mass parameters tested on the model of a swept-wing airplane design. (Points are for loadings listed in table II.)

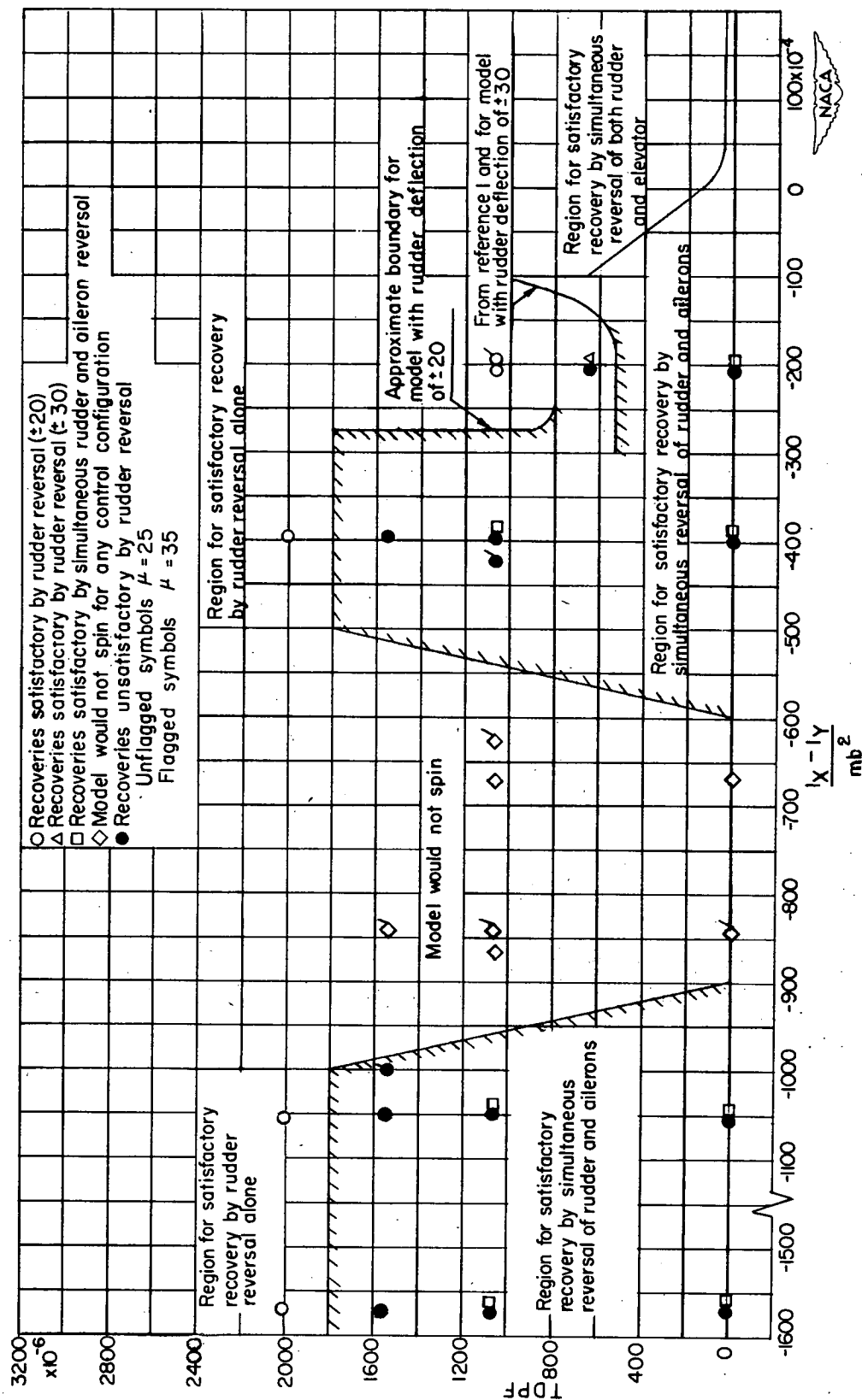


Figure 6.- Spin-recovery requirements for a swept-wing airplane design.